Biogenic volatile organic compound ambient mixing ratios and emission rates in the Alaskan Arctic tundra

Hélène Angot[1], Katelyn McErlean[1], Lu Hu[2], Dylan B. Millet[3], Jacques Hueber[1], Kaixin Cui[1], Jacob Moss[1], Catherine Wielgasz[2], Tyler Milligan[1], Damien Ketcherside[2], Marion Syndonia Bret-Harte[4], Detlev Helmig[1]

[1]Institute of Arctic and Alpine Research, University of Colorado Boulder, Boulder, CO, USA.

[2]Department of Chemistry and Biochemistry, University of Montana, Missoula, MT, USA.

[3]Department of Soil, Water, and Climate, University of Minnesota, Minneapolis-Saint Paul, MN, USA.

[4]Institute of Arctic Biology, University of Alaska-Fairbanks, Fairbanks, Alaska, USA.

Abstract

Rapid Arctic warming, a lengthening growing season, and increasing abundance of biogenic volatile organic compounds (BVOC)-emitting shrubs are all anticipated to increase atmospheric BVOCs in the Arctic atmosphere, with implications for atmospheric oxidation processes and climate feedbacks. Quantifying these changes requires an accurate understanding of the underlying processes driving BVOC emissions in the Arctic. While boreal ecosystems have been widely studied, little attention has been paid to Arctic tundra environments. Here, we report terpenoid (isoprene, monoterpenes, and sesquiterpenes) ambient mixing ratios and emission rates from key dominant vegetation species at Toolik Field Station (TFS; 68°38'N, 149°36'W) in northern Alaska during two back-to-back field campaigns (summers 2018 and 2019) covering the entire growing season. Isoprene ambient mixing ratios observed at TFS fell within the range of values reported in the Eurasian taiga (0-500 pptv), while monoterpene and sesquiterpene ambient mixing ratios were respectively close to and below the instrumental quantification limit (~2 pptv). Isoprene surface emission rates ranged from 0.2 to 2250 μgC/m^2/h (mean of 85 μgC/m^2/h) and monoterpene emission rates remained on average below 1 μgC/m^2/h over the course of the study. We further quantified the temperature dependence of isoprene emissions from local vegetation including *Salix* spp. (a known isoprene emitter), and compared the results to predictions from the Model of Emissions of Gases and Aerosols from Nature version 2.1 (MEGAN2.1). Our observations suggest a 180-215% emission increase in response to a 3-4°C warming and the MEGAN2.1 temperature algorithm exhibits a close fit with observations for enclosure temperatures in the 0-30°C range. The data presented here provide a baseline to investigate future changes in the BVOC emission potential of the under-studied Arctic tundra environment.

1. Introduction

As a major source of reactive carbon to the atmosphere, biogenic volatile organic compounds (BVOCs) emitted from vegetation play a significant role in global carbon and oxidation cycles (Fehsenfeld et al., 1992). Global emission estimates of BVOCs are in the range of 700-1100 TgC per year, ~70-80% of which corresponds to terpenoid species: isoprene, monoterpenes (MT), and sesquiterpenes (SQT) (Guenther et al., 1995, 2006; Sindelarova et al., 2014). Despite their relatively short atmospheric lifetimes (a few minutes to 1 day for terpenoids), BVOCs affect climate through their effects on the hydroxyl radical (OH, which dictates the lifetime of atmospheric methane), tropospheric ozone (O_3, a key greenhouse gas), and aerosols (which influence radiative scattering) (Arneth et al., 2010; Fuentes et al., 2000; Peñuelas and Staudt, 2010). The oxidation of those BVOCs also drives the formation of secondary organic aerosols (SOA) through both gas- and aqueous-phase mechanisms (Carlton et al., 2009; Lim et al., 2005). The potential for increased SOA formation, expected to result in climate cooling (Kulmala et al., 2004), complicates the climate feedbacks of BVOC emissions (Tsigaridis and Kanakidou, 2007; Unger, 2014).

Global models of BVOC emissions assume minimal emissions from the Arctic due to low leaf area index and relatively cold temperatures (Guenther et al., 2006; Sindelarova et al., 2014). However, this assumption relies on few observations and has been increasingly challenged by field data (Tang et al., 2016). Recent measurements have revealed significant BVOC emissions from Arctic tundra and vegetation, including *Sphagnum* mosses, wetland sedges, and dwarf shrubs (Ekberg et al., 2009, 2011; Faubert et al., 2010; Holst et al., 2010; Lindfors et al., 2000; Potosnak et al., 2013; Rinnan et al., 2011; Schollert et al., 2014; Tiiva et al., 2008). These results are of importance because BVOC emissions are expected to increase in the Arctic due to climate warming and associated vegetation and land cover change (Faubert et al., 2010; Potosnak et al., 2013; Rinnan et al., 2011; Tiiva et al., 2008). Field warming studies have shown strong increases in BVOC emissions from shrub heath (Michelsen et al., 2012; Tiiva et al., 2008). Furthermore, the temperature dependence of Arctic BVOC fluxes appears to be significantly greater than for tropical and subtropical ecosystems (Holst et al., 2010; Rinnan et al., 2014), with up to 2-fold increases in MT emissions and 5-fold increases in SQT emissions by subarctic heath for a 2°C warming (Valolahti et al., 2015). Similarly, Kramshøj et al. (2016) and Lindwall et al. (2016) examined the

response of BVOC emissions to an experimental 3-4°C warming and reported a 260-280% increase in total emissions. Together, the above results emphasize the strong temperature sensitivity of BVOC emissions from Arctic ecosystems.

Changing BVOC emissions in the Arctic due to climate and land cover shifts can thus be expected to perturb the overall oxidative chemistry of the region. Previous studies have hypothesized that BVOCs might already impact the diurnal cycle of ozone in the Arctic boundary layer (Van Dam et al., 2016). Changing BVOC emissions can also further affect climate through various feedback mechanisms; Quantifying these changes requires an accurate understanding of the underlying processes driving BVOC emissions in the Arctic. While BVOC ambient mixing ratios and emission rates have been studied in boreal ecosystems, less attention has been paid to Arctic tundra environments (Lindwall et al., 2015). Here, we report BVOC ambient mixing ratios and emission rates at Toolik Field Station (TFS) in the Alaskan Arctic. This study builds on the previous isoprene study at TFS by Potosnak et al. (2013), while also providing a major step forward from that work. In particular, we present the first continuous summertime record of ambient BVOCs (including isoprene and MT) and their first-generation oxidation products in the Arctic tundra environment. The data presented here provide a baseline to investigate future changes in the BVOC emission potential of the under-studied Arctic tundra environment. Due to increasing shrub prevalence across northern Alaska (Berner et al., 2018; Tape et al., 2006), as well as the Eurasian (Macias-Fauria et al., 2012) and Russian Arctic (Forbes et al., 2010), the results of this study have significance to tundra ecosystems across a vast region of the Arctic. We further compare the observed temperature dependence of isoprene emissions with predictions from the Model of Emissions of Gases and Aerosols from Nature version 2.1 (MEGAN2.1), a widely used modeling framework for estimating ecosystem-atmosphere BVOC fluxes (Guenther et al., 2012).

2. Material and Methods

2.1 Study site

This study was carried out at TFS, a Long-Term Ecological Research (LTER) site located in the tundra on the north flank of the Brooks Range in northern Alaska (68°38'N, 149°36'W; see Fig.1). Vegetation speciation and dynamics, and their changes over time, have been well documented at the site. *Betula* (birch) and *Salix* (willow) are the most common deciduous shrubs (Kade et al., 2012). Common plant species include *Betula nana* (dwarf birch), a major player in ongoing Arctic

greening (Hollesen et al., 2015; Sistla et al., 2013), *Rhododendron tomentosum* (formerly *Ledum palustre*; Labrador tea); *Vaccinium vitis-idaea* (lowbush cranberry), *Eriophorum vaginatum* (cotton grass), *Sphagnum angustifolium* (peat moss), *Alectoria ochroleuca* (witches hair lichen), and many other perennial species of Carex, mosses, and lichens. Vegetation cover at this site is classified as tussock tundra (see Fig.1), which is the most common vegetation type in the northern foothills of the Brooks Range (Elmendorf et al., 2012; Kade et al., 2012; Shaver and Chapin, 1991; Survey, 2012; Walker et al., 1994).

Emission measurements and atmospheric sampling were conducted from a weatherproof instrument shelter located ~350 m to the west of TFS (see Fig.S.I.1). Winds at TFS are predominantly from the southerly and northerly sectors (Toolik Field Station Environmental Data Center, 2019), minimizing any influence from camp emissions at the site. Two field campaigns were carried out: the first from mid-July to mid-August 2018, and the second from mid-May to the end of June 2019. These two back-to-back campaigns cover the entire growing season (Sullivan et al., 2007), from the onset of snow melt mid-May to the first snow fall mid-August.

2.2 Ambient online measurements of BVOCs and their oxidation products

2.2.1 Gas chromatography and mass spectrometry with flame ionization detector (GC-MS/FID)

An automated GC-MS/FID system was deployed for continuous measurements of atmospheric BVOCs at ~2-hour time resolution during the 2018 and 2019 field campaigns. In addition, the system was operated remotely following the 2018 campaign (through September 15th) to collect background values at the beginning of autumn. Air was pulled continuously from an inlet on a 4 m meteorological tower located approximately 30 m from the instrument shelter (Van Dam et al., 2013). Air passed through a sodium thiosulfate-coated O_3 scrubber for selective O_3 removal – to prevent sampling losses and artifacts for reactive BVOCs (Helmig, 1997; Pollmann et al., 2005) – and through a moisture trap to dry the air to a dew point of -45°C. The moisture trap was a U-shaped SilcoSteel^{TM} tube (stainless steel treated) cooled using thermoelectric coolers. Analytes were concentrated on a Peltier-cooled (-40°C) multistage micro-adsorbent trap (50 % Tenax-GR and 50 % Carboxen 1016). Analysis was accomplished by thermal desorption and injection for cryogen free GC using a DB-1 column (60 m × 320 μm × 5 μm) and helium as carrier gas. The oven temperature was set to 40°C for 6 minutes, then increased to 260°C at 20°C/min, and held

isothermally at 260°C for 13 minutes. The column flow was split between an FID and a MS for simultaneous quantification and identification. Blanks and calibration standards were regularly injected from a manifold. Isoprene (*m/z* 67 and 68), methacrolein (MACR) and methylvinylketone (MVK) (*m/z* 41, 55, and 70), MT (*m/z* 68, 93, 121, and 136), and SQT (*m/z* 204, 91, 93, 119, and 69) were identified and quantified using the MS in selected ion-monitoring mode (SIM). The response to isoprene was calibrated using a primary gas standard supplied by the National Physical Laboratory (NPL), certified as containing 4.01±0.09 ppb of isoprene in a nitrogen matrix. The analytical uncertainty for isoprene was estimated at 16 % based on the certified uncertainty of the standard and on the repeatability of standard analysis throughout the campaigns. Instrument responses for MACR, MVK, α-pinene, and acetonitrile were calibrated with multi-component standards containing 1007 ppb MACR, 971 ppb MVK, 967 ppb α-pinene, and 1016 ppb acetonitrile (Apel-Riemer Environmental Inc., Miami, FL, USA) dynamically diluted into a stream of ultra-zero grade air to ~3 ppb. Quantification of other terpenoid compounds was based on GC peak area (FID response) plus relative response factors using the effective carbon number concept (Faiola et al., 2012; Scanlon and Willis, 1985). The limit of quantification (LOQ) was ~2 pptv (pmol/mol by volume). In order to monitor and correct for long-term trends in the detection system, including detector drift and decreasing performance of the adsorbent trap, we used peak areas for long-lived chlorofluorocarbons (CFCs) that were monitored in the air samples together with the BVOCs as an internal reference standard. The atmospheric trace gases CCl_3F (CFC-11) and $CCl_2FCCl_2F_2$ (CFC-113) are ideal in this regard because they are ubiquitous in the atmosphere and exhibit little spatial and temporal variability (Karbiwnyk et al., 2003; Wang et al., 2000).

2.2.2 Proton-Transfer-Reaction Time-of-Flight Mass-Spectrometry (PTR-ToF-MS)

During the summer 2019 campaign, isoprene mixing ratios in ambient air were also measured by PTR-ToF-MS (model 4000, Ionicon Analytik GmbH, Innsbruck, Austria). The sample inlet was located on the 4 m meteorological tower, right next to the GC-MS/FID inlet. In brief, ambient air was continuously pulled through the PTR-ToF-MS drift-tube, where VOCs with proton affinities higher than that of water (>165.2 kcal/mol) were ionized via proton-transfer reaction with primary H_3O^+ ions, then subsequently separated and detected by a time-of-flight mass spectrometer (with a mass resolving power up to 4000). At TFS, the PTR-ToF-MS measured ions from 17–400 *m/z* every 2 minutes. Ambient air was drawn to the instrument at 10–15 L/min via ~30 m of 1/4" O.D.

PFA tubing maintained at ~55°C, and then subsampled by the instrument through ~100 cm of 1/16" O.D. PEEK tubing maintained at 60°C. The residence time from the inlet on the 4 m meteorological tower to the drift-tube was less than 5 seconds. Instrument backgrounds were quantified approximately every 5 hours for 20 minutes during the campaign by measuring VOC-free air generated by passing ambient air through a heated catalytic converter (375 °C, platinum bead, 1 % wt. Pt, Sigma Aldrich). Calibrations were typically performed every 4 days via dynamic dilution of certified gas standard mixtures containing 25 distinct VOCs including isoprene (Apel-Riemer Environmental Inc., Miami, FL, USA). Here, we report isoprene mixing ratios to inter-compare with GC-MS measurements; other species will be reported in future work. The measurement uncertainty for isoprene is ~25%, which includes uncertainties in the gas standards, calibration method, and data processing.

2.2.3 Instrument inter-comparison

Figure S.I.2 shows a comparison of the GC-MS and PTR-ToF-MS isoprene mixing ratios in ambient air. With a correlation coefficient of 0.93 and a linear regression slope of 0.7-1.0, the two measurements agreed within their combined measurement uncertainties, in line with earlier inter-comparison studies (e.g., Dunne et al., 2018; de Gouw et al., 2003). Similarly, we found a correlation coefficient of 0.96 between GC-MS and PTR-ToF-MS MVK+MACR mixing ratios (not shown). The good agreement between these two independent techniques gives us confidence that the ambient air results presented here are robust.

2.3 Ambient air vertical profiles

Vertical isoprene mixing ratio profiles were obtained using a 12-foot diameter SkyDoc tethered balloon. A total of eight vertical profiles were performed at ~3-hour intervals between 12:30 pm Alaska Standard Time (AST) on June 15, 2019 and 11:00 am AST on June 16, 2019 in order to capture a full diurnal cycle (solar noon around 2 pm AST). Sampling packages were connected to the tether line such that resulting sampling heights were ~30, ~100, ~170, and ~240 m above ground level. One identical sampling package was deployed at the surface. Each sampling package contained an adsorbent cartridge for sample collection (see below) connected to a downstream battery-powered SKC pocket pump controlled using a mechanical relay, a programmable Arduino, and a real-time clock. Once the balloon reached its apex (~ 250-300 m a.g.l.), the five pumps were activated simultaneously and samples collected for 30 minutes to ensure that enough material was

collected. It should be noted that changes in wind speed and turbulence during the 30-min sampling period often affected the shape of the tethered line and the sampling altitude adding further uncertainty to the vertical profiles presented here. At the end of the 30-min sampling period, the balloon was brought back down. The adsorbent cartridges were prepared in house using glass tubing (89 mm long × 6.4 mm outer diameter, 4.8 mm inner diameter), and loaded with Tenax-GR and Carboxen 1016 adsorbents (270 mg of each), following established practice (Ortega and Helmig, 2008 and references therein). An inlet ozone scrubber was installed on each cartridge to prevent BVOC sampling losses. Field blanks were collected by opening a cartridge (with no pumped airflow) during each balloon flight. Following collection, adsorbent cartridges were sealed with Teflon-coated brass caps and stored in the dark at ~4°C until chemical analysis. Samples were analyzed at the University of Colorado Boulder following the method described in S.I. Section 1. Our previous inter-comparison of this cartridge-GC-MS/FID method with independent and concurrent PTR-MS observations showed that the two measurements agree to within their combined uncertainties at ~25% (Hu et al., 2015). Meteorological conditions were monitored and recorded during each balloon flight with a radiosonde (Met1, Grant Pass, OR, USA) attached to the tethered line just below the balloon.

2.4 BVOC emission rates

2.4.1 Dynamic enclosure measurements

We used dynamic enclosure systems operated at low residence time to quantify vegetative BVOC emissions following the procedure described by Ortega et al. (2008) and Ortega and Helmig (2008). Two types of enclosures were used: branch and surface chambers. For branch enclosures, a Tedlar® bag (Jensen Inert Products, Coral Springs, FL) was sealed around the trunk side of a branch. For surface enclosures, the bag was placed around a circular Teflon® base (25 cm wide × 16 cm height; see Fig. 2). For both branch and surface enclosures, the bag was connected to a purge-air line and a sampling line, and positioned around the vegetation minimizing contact with foliage. While purging the enclosure (see Section 2.4.3), the vegetation was allowed to acclimate for 24 hours before BVOC sampling began. Samples were collected from the enclosure air, concentrated onto solid-adsorbent cartridges (see Section 2.3) with an automated sampler, and analyzed in-laboratory at the University of Colorado Boulder following the campaign (see S.I. Section 1). Temperature and relative humidity were recorded inside and outside the enclosure (see

Fig. 2; S-THB-M002 sensors, Onset HOBO, Bourne, MA, USA) with a data logger (H21-USB, Onset HOBO, Bourne, MA, USA). Additionally, photosynthetically active radiation (400-700 nm; S-LIA-M003, Onset HOBO, Bourne, MA, USA) was measured inside the enclosure. Once installed, enclosures were operated for 2-10 days. The tundra vegetation around TFS is heterogeneous but most dominant species (except *Rubus chamaemorus*) were sampled. Table 1 presents the median relative percent cover of plant species in LTER experimental control plots at TFS (Gough, 2019) and indicates whether plant species were present in surface or bag enclosures. The complete list of species sampled and pictures of the enclosures are available in Figures S.I.3-S.I.15; the two sampling sectors are highlighted in Fig.S.I.1. Surface enclosures were divided into three vegetation types: *Salix* spp. (high isoprene emitter), *Betula* spp. (e.g., *Betula nana* dominance), and miscellaneous (mix of different species, including lichens and mosses).

2.4.2 Emission rates

The emission rate (ER in µgC/m^2/h) for surface enclosures was calculated as follows:

$$ER_{surface} = \frac{(C_{out} - C_{in})Q}{S}, \quad (1)$$

where C_{in} and C_{out} are the inlet and outlet analyte concentrations (in µgC/L), Q is the purge air flow rate (in L/h), and S the surface area of the enclosure (in m^2).

The ER for branch enclosures (in µgC/g/h) was calculated as follows:

$$ER_{branch} = \frac{(C_{out} - C_{in})Q}{m_{dry}}, \quad (2)$$

where m_{dry} is the dried mass (in g) of leaves enclosed, determined by drying the leaves – harvested after the experiment – at 60-70°C until a consistent weight was achieved (Ortega and Helmig, 2008).

Emission rates were standardized to 30°C and to a PAR level of 1000 µmol/m^2/s using the algorithms described in Guenther et al. (1993, 1995).

2.4.3 Enclosure purge air

Purge air was provided by an upstream high-capacity oil-free pump providing positive pressure to the enclosure, and equipped with an in-line O_3 scrubber to avoid loss of reactive BVOCs from

reaction with O_3 in the enclosure air and during sampling (Helmig, 1997; Pollmann et al., 2005). The purge flow was set to 25 L/min and regularly checked using a volumetric flow meter (Mesa Labs Bios DryCal Defender, Butler, NJ, USA). Excess air escaped from the open end (tied around the Teflon® base) while the sample air flow was pulled into the sampling line (see below).

2.4.4 Sample collection

A continuous airflow of 400-500 mL/min was drawn from the enclosure through the sampling line. A fraction of this flow was periodically collected at 265-275 mL/min on adsorbent cartridges (see Section 2.3) using a 10-cartridge autosampler (Helmig et al., 2004). During sampling, cartridges were kept at 40°C, *i.e.,* above ambient temperature, to prevent water accumulation on the adsorbent bed (Karbiwnyk et al., 2002). Samples were periodically collected in series to verify lack of analyte breakthrough. Time-integrated samples were collected for 120 min every 2 hours to establish diurnal cycles of BVOC emission. Upon collection, samples were stored in the dark at ~4°C until chemical analysis back at the University of Colorado Boulder.

2.4.5 Internal standards

In order to identify potential BVOC losses during transport, storage, and chemical analysis, 255 of the employed cartridges were pre-loaded with a four-compound standard mixture prior to the field campaigns. These internal standard compounds (toluene, 1, 2, 3-trimethylbenzene, 1, 2, 3, 4-tetrahydronaphtalene, and 1, 3, 5-triisopropylbenzene) were carefully chosen to span a wide range of volatility (C_7-C_{15}) and to not interfere (*i.e.,* coelute) with targeted BVOCs. The recovery of these four compounds was assessed at the end of the campaign, following the analytical procedure described in S.I. Section 1. Recovery rates were 101.8 ± 13.5 % (toluene), 95.2 ± 20.1 % (1,2,3-trimethylbenzene), 95.6 ± 26.6 % (1,2,3,4-tetrahydronaphtalene), and 100.9 ± 18.7 % (1,3,5-triisopropylbenzene). These results indicate that, overall, BVOC losses during transport, storage, and chemical analysis were negligible. Ortega et al. (2008) previously evaluated systematic losses of analytes to enclosure systems similar to those used here. The same four-component standard was introduced into the purge air flow of the enclosures to quantify losses as a function of volatility. That work found median losses of MT and SQT on the order of 20-30%. The emission rates presented here are therefore possibly biased low by a similar amount.

2.5 Peak fitting algorithm

The analysis of ambient air and enclosure chromatograms was performed using the TERN (Thermal desorption aerosol GC ExploreR and iNtegration package) peak fitting tool implemented in Igor Pro and available online at https://sites.google.com/site/terninigor/ (Isaacman-VanWertz et al., 2017).

2.6 Ancillary parameters

Meteorological parameters. A suite of meteorological instruments was deployed on the 4 m tower. Wind speed and direction were measured at ~4 m above ground level with a Met One 034B-L sensor. As described by Van Dam et al. (2013), temperature was measured at three different heights using RTD temperature probes (model 41342, R.M. Young Company, Traverse City, MI) housed in aspirated radiation shields (model 43502, R.M. Young Company, Traverse City, MI). Regular same-height inter-comparisons were conducted to test for instrumental offsets. Incoming and reflected solar radiation were recorded with LI200X pyranometers (Campbell Scientific Instruments).

In addition, historical (1988-2019) meteorological data recorded by TFS Environmental Data Center are available at: https://toolik.alaska.edu/edc/abiotic_monitoring/data_query.php

Particle measurements. A Met One Instruments Model 212-2 8-channel (0.3 to 10 µm) particle profiler was operated continuously on the roof of the weatherproof instrument shelter. This instrument uses a laser-diode based optical sensor and light scatter technology to detect, size, and count particles (http://mail.metone.com/particulate-Aero212.htm).

Nitrogen oxides. Nitrogen oxides (NO_x) were measured with a custom-built, high sensitivity (~5 pptv detection limit) single-channel chemiluminescence analyzer (Fontijn et al., 1970). The instrument monitors nitric oxide (NO) and nitrogen dioxide (NO_2) in ambient air using a photolytic converter. Automated switching valves alternated between NO and NO_2 mode every 30 minutes. Calibration was accomplished by dynamic dilution of a 1.5 ppm compressed NO gas standard (Scott-Marrin, Riverside, CA, USA).

2.7 Theoretical response of isoprene emissions to temperature in MEGAN2.1

We applied our isoprene emission measurements to evaluate the temperature response algorithms embedded in MEGAN2.1 (Guenther et al., 2012). Theoretical isoprene emission rates (F_T) were calculated for TFS as:

$$F_T = C_{CE}\,\gamma_T \sum_j \varkappa_j\,\varepsilon_j \quad (3)$$

where C_{CE} is the canopy environment coefficient (assigned a value that results in γ_T = 1 under standard conditions), and ε_j is the emission factor under standard conditions for vegetation type j with fractional grid box areal coverage $\varkappa_j$. We used $\sum_j \varkappa_j\,\varepsilon_j$ = 2766 µg/m^2/h at TFS based on the high resolution (1 km) global emission factor input file available at https://bai.ess.uci.edu/megan/data-and-code/megan21. The temperature activity factor (γ_T) was calculated as:

$$\gamma_T = E_{opt} \times \frac{200\,e^{95\,x}}{200 - 95 \times (1 - e^{200\,x})} \quad (4)$$

with

$$x = \frac{\frac{1}{T_{opt}} - \frac{1}{T}}{0.00831} \quad (5)$$

$$E_{opt} = 2 \times e^{0.08(T_{10} - 297)} \quad (6)$$

$$T_{opt} = 313 + 0.6(T_{10} - 297), \quad (7)$$

where T is the enclosure ambient air temperature and T_{10} the average enclosure air temperature over the past 10 days.

3. Results and Discussion

3.1 Ambient air mixing ratios

3.1.1 Isoprene and oxidation products

Figure 3 (top panels) shows the time-series of isoprene mixing ratios in ambient air recorded over the course of this study at TFS with the GC system. Mixing ratios were highly variable and ranged from below the quantification limit to 505 pptv (mean of 36.1 pptv). The PTR-ToF-MS gave similar results (see Fig.S.I.16a). These mixing ratios fall within the range of values reported in the Eurasian taiga (e.g., Hakola et al., 2000, 2003; Lappalainen et al., 2009). For example, Hakola et

al. (2003) reported a maximum monthly mean mixing ratio of 98 pptv (in July) in Central Finland while Hakola et al. (2000) observed mixing ratios ranging from a few pptv to ~600 pptv in Eastern Finland. In general, however, BVOC emissions in the Eurasian taiga are relatively low compared to forest ecosystems in warmer climates and are dominated by monoterpenes (Rinne et al., 2009).

Isoprene mixing ratios peaked on August 1, 2018 around 4 pm and on June 20, 2019 around 10 pm, respectively. These two peaks occurred 3-5 hours after the daily maximum ambient temperature was reached (17.8°C in 2019 and 21.8°C in 2019 – see Fig. 3). The isoprene peak on June 20, 2019 was concomittant with enhanced acetonitrile mixing ratios and particle counts (see Fig. 4), reflecting unusually hazy conditions that day at TFS. We attribute the particle and acetonitrile enhancements to intense wildfires occurring across the Arctic Circle at that time – most of them in southern Alaska and Siberia (Earth Observatory, 2019). Acetonitrile increased by a factor of 4 during this event, compared to a factor of 21 increase for isoprene. The higher emission factor for acetonitrile *vs.* isoprene from biomass burning in boreal forests (Akagi et al., 2011) and the relatively short lifetime of isoprene (Atkinson, 2000) indicate that the observed isoprene enhancement was due to fresh local biogenic emissions rather than transported wildfire emissions.

Over the course of this study, we recorded MACR and MVK mixing ratios respectively ranging from below the quantification limit to 95 pptv (12.4 ± 16.1 pptv; mean ± standard deviation) and from below the quantification limit to 450 pptv (43.1 ± 66.7 pptv; see Fig. 3, top panels). The PTR-ToF-MS gave similar results (see Fig.S.I.16b). Median NO and NO_2 mixing ratios of 21 and 74 pptv, respectively, during the 2019 campaign (not shown) suggest a low-NO_x environment, in line with previous studies at several Arctic locations (Bakwin et al., 1992; Honrath and Jaffe, 1992). Under such conditions, MACR and MVK mixing ratios should be used as upper estimates as it has been noted that some low-NO_x isoprene oxidation products (isoprene hydroxyhydroperoxides) can undergo rearragement in GC and PTR-MS instruments and be misidentified as MACR and MVK (Rivera-Rios et al., 2014). We found a high correlation between MACR and MVK ($R^2 = 0.95$, $p < 0.01$) and between these two compounds and isoprene ($R^2 \sim 0.80$, $p < 0.01$). Increases of MACR and MVK mixing ratios above the background were mostly concomitant with isoprene increases, suggesting that atmospheric or within-plant oxidation of isoprene was their main source (Biesenthal et al., 1997; Hakola et al., 2003; Jardine et al., 2012). The mean ratio of MVK to MACR was 2.7, within the range reported by earlier studies (e.g., Apel et al., 2002; Biesenthal and

Shepson, 1997; Hakola et al., 2003; Helmig et al., 1998), and no clear diurnal cycle in the ratio was found. This record of ambient air isoprene, MACR, and MVK mixing ratios is, to the best of our knowledge, the first in an Arctic tundra environment. The combined measurement of isoprene and its oxidation products provides a new set of observations to further constrain isoprene chemistry under low-NO_x conditions in atmospheric models (e.g., Bates and Jacob, 2019).

3.1.2 Isoprene vertical profiles

Figure 5 shows vertical profiles (0 to ~250 m a.g.l.) of isoprene mixing ratios derived from the 30-min tethered balloon samples collected on June 15 and 16, 2019. Temperature profiles (see Fig.S.I.17) indicate that most of the flights were performed in a convective boundary layer (Holton and Hakim, 2013). A nocturnal boundary layer was, however, observed in the first ~50 m from ~2 am to ~4:30 am (see Fig.S.I.17e-f) – with temperature increasing with elevation.

Except during the last flight, isoprene mixing ratios were in the range of background levels (~0-50 pptv) reported with the GC-MS (see Section 3.1.1). Samples collected from 10-10:30 am on June 16 (see Fig. 5h) showed a pronounced gradient, with 200 pptv at ground level and decreasing mixing ratios with elevation. This maximum at ground-level is expected for a VOC with a surface source (Helmig et al., 1998) while the 200 pptv mixing ratio can likely be attributed to a temperature-driven increase of isoprene emissions by the surrounding vegetation. Indeed, the ambient temperature at ground-level was higher during that flight than during the previous ones (see Fig.S.I.17h). The diurnal cycles of isoprene emissions and temperature are further discussed in Section 3.2.2. Interestingly, the GC-MS and the PTR-ToF-MS did not capture this 200 pptv maximum (see Fig. 3 and Fig.S.I.16), which may be because the balloon flights were performed at a different location (near sampling sector B, see Fig.S.I.1) surrounded by a higher fraction of isoprene-emitting shrubs (willow).

Samples collected on June 16, 2019 from 4 to 4:30 am (see Fig. 5f) show decreasing isoprene mixing ratios with increasing elevation, suggesting higher levels (25-50 pptv) in the nocturnal boundary layer than above. This result suggests continuing isoprene emissions by the surrounding vegetation under low-PAR conditions. This is further discussed in Section 3.2.2.

3.1.3 Monoterpenes and Sesquiterpenes

MT mixing ratios ranged from 3 to 537 pptv (14 ± 18 pptv; median ± standard deviation) during the 2019 campaign according to the PTR-ToF-MS measurements. Using the GC-MS/FID, we were able to detect and quantify the following MT in ambient air: α-pinene, camphene, sabinene, p-cymene, and limonene. Mean mixing ratios are reported in Table 2 (for values lower than the LOQ, mixing ratios equal to half of the LOQ are used). These compounds have been previously identified as emissions of the widespread circumpolar dwarf birch *Betula nana* (Li et al., 2019; Vedel-Petersen et al., 2015) and other high Arctic vegetation (Schollert et al., 2014). The quantification frequency of camphene, sabinene, p-cymene, and limonene was low (see Table 2) and MT mixing ratios in ambient air were dominated by α-pinene. Several prior studies performed at boreal sites have similarly identified α-pinene as the most abundant monoterpene throughout the growing season (e.g., Hakola et al., 2000; Lindfors et al., 2000; Spirig et al., 2004; Tarvainen et al., 2007). We did not detect any sesquiterpene in ambient air above the 2 pptv instrumental LOQ.

Overall, isoprene and α-pinene dominated the ambient air BVOC profile at TFS, respectively constituting ~72% and ~24% of total BVOCs quantified in ambient air (on a mixing-ratio basis).

3.2 Emission rates

3.2.1 Branch enclosures

A branch enclosure experiment was performed from July 27 to August 2, 2018 on *Salix glauca* to investigate BVOC emission rates per dry weight plant biomass (see Fig.S.I.5). Isoprene emission rates ranged from <0.01 to 11 µgC/g/h (with a mean enclosure temperature of 16.5°C and mean PAR of 880 µmol/m^2/s), in line with non-normalized emission rates reported at Kobbefjord, Greenland by Kramshøj et al. (2016; Supplementary Table 5) for the same species under slightly different environmental conditions (mean temperature of 24.6°C and mean PAR of 1052 µmol/m^2/s). Once standardized to 30°C and 1000 µmol/m^2/s, our emission rates averaged 5 µgC/g/h, in good agreement with standardized emissions reported at Kobbefjord (mean of 7 µgC/g/h) by Vedel-Petersen et al. (2015). The quantified MTs had emissions averaging two orders of magnitude lower than those of isoprene (0.01 vs 1 µgC/g/h). Emission rates for the sum of α-pinene, β-pinene, limonene, camphene, and 1,8-cineole ranged from <0.01 to 0.06 µgC/g/h. These results are again in good agreement with those reported for the same species at Kobbefjord (~0.01 µgC/g/h) by Kramshøj et al. (2016; Supplementary Table 5).

3.2.2 Surface emission rates

The isoprene surface emission rate, as inferred from surface enclosures, was highly variable and ranged from 0.2 to ~2250 μgC/m^2/h (see Fig. 6). The 2250 μgC/m^2/h maximum, reached on June 26, 2019, with an enclosure temperature of 32°C, is higher than maximum values reported at TFS by Potosnak et al. (2013) (1200 μgC/m^2/h at an air temperature of 22°C). It should be noted that these maximum values were observed at different ambient temperatures; we further investigate the temperature dependency of isoprene emissions in Section 3.3. Elevated surface emission rates (*i.e.,* > 500 μgC/m^2/h) were all observed while sampling enclosures dominated by *Salix* spp.. At TFS, the overall 24-hour mean isoprene emission rate amounted to 85 μgC/m^2/h, while the daytime (10 am-8 pm) and midday (11 am-2 pm) means were 140 and 213 μgC/m^2/h, respectively. To put this in perspective, the average isoprene surface emission rate standardized to 30°C and 1000 μmol/m^2/s (~ 300 μgC/m^2/h) was an order of magnitude lower than emission rates reported for warmer mid-latitude or tropical forests. For example, average midday fluxes of 3000 μgC/m^2/h were reported in a northern hardwood forest in Michigan (Pressley et al., 2005), while several reports of isoprene emissions from tropical ecosystems give daily estimates of 2500-3000 μgC/m^2/h (Helmig et al., 1998; Karl et al., 2004; Rinne et al., 2002).

Figure 7 shows the measured surface emission rates for α-pinene, β-pinene, limonene, and 1,8-cineole. While p-cymene, sabinene, 3-carene, and isocaryophyllene (SQT) were detected in some of the surface enclosure samples, we focus the discussion on the most frequently quantified compounds. It is worth noting that the most frequently observed compounds in enclosure samples are among the most frequently seen MT in ambient air (see Section 3.1.3). Regardless of the species, emission rates remained on average below 1 μgC/m^2/h over the course of the study (see Table 3). These results are at the low end of emission rates reported for four vegetation types in high Arctic Greenland (Schollert et al., 2014), but in line with results reported at Kobbefjord, Greenland by Kramshøj et al. (2016; Supplementary Table 4).

Figures 8a-c show the mean diurnal cycle (over the two campaigns) of isoprene surface emission rates for different vegetation types (see Fig.S.I.3-15 for nomenclature). The two field campaigns were carried out during the midnight sun period, which could possibly sustain BVOC emissions during nighttime. It should, however, be noted that low sun angles translate to very low PAR and a typical diurnal pattern is observed in summer at TFS despite 24 hours of light (see Fig. 8h). Regardless of the vegetation type, isoprene emission rates exhibited a significant diurnal cycle

with an early afternoon maximum, in line with the mean diurnal cycle of enclosure temperature and PAR. These results are in line with the well-established diurnal variation of BVOC emissions in environments ranging from Mediterranean to boreal forests (e.g., Fares et al., 2013; Liu et al., 2004; Ruuskanen et al., 2005; Zini et al., 2001) and with the correlation between isoprene ambient air mixing ratios and temperature at TFS (see Section 3.1). Despite the relatively low MT emission rates, a significant diurnal cycle was also observed with peak total MT emissions of ~1 μgC/m^2/h during early afternoon for both *Salix* spp. and *Betula* spp. (Fig. 8e-f). A summary of emission rates per vegetation type and time of day is given in Table 3. As can be seen in Table 3 and Fig. 8, PAR and BVOC emissions significantly decreased at night but were still detectable. These sustained BVOC emissions during nighttime confirm observations by Lindwall et al. (2015) during a 24-hour experiment with five different Arctic vegetation communities and explain the higher isoprene levels observed in the nocturnal boundary layer than above during the diurnal balloon experiment (see Section 3.1.2).

The ratio of total MT (given by the sum of α-pinene, β-pinene, limonene, and 1,8-cineole) emissions to isoprene emissions was an order of magnitude higher for *Betula* spp. (0.22) than for *Salix* spp. (0.03). This result, driven by the relatively lower isoprene emissions of *Betula* spp., is in line with earlier studies, suggesting similar emission characteristics for Arctic plants (e.g., Kramshøj et al., 2016; Vedel-Petersen et al., 2015).

4. Insights into future changes

4.1 Response of isoprene emissions to temperature

The Arctic has warmed significantly during the last three decades and temperatures are projected to increase an additional 5-13°C by the end of the century (Overland et al., 2014). Heat wave frequency is also increasing in the terrestrial Arctic (Dobricic et al., 2020). For example, western Siberia experienced an unusually warm May in 2020, with temperatures of 20-25°C (Freedman and Cappucci, 2020). In that context, numerous studies have pointed out the likelihood of increased BVOC emissions due to Arctic warming and associated vegetation and land cover change (Faubert et al., 2010; Potosnak et al., 2013; Rinnan et al., 2011; Tiiva et al., 2008).

Over the course of the two field campaigns at TFS, BVOC surface emission rates were measured over a large span of enclosure temperatures (2-41°C). While isoprene and MT emissions respond to leaf temperature (Guenther et al., 1993), air temperature was used here in place of leaf

464 temperature – which has been assumed before in the literature for high-latitude ecosystems (e.g.,
465 Olofsson et al., 2005; Potosnak et al., 2013). Several studies have, however, suggested a
466 decoupling of leaf and air temperature in tundra environments (Lindwall et al., 2016; Potosnak et
467 al., 2013). With predicted increase of air temperature in the Arctic, it still remains largely unknown
468 how leaf temperature will change and impact BVOC emissions. As suggested by Tang et al.
469 (2016), long-term parallel observations of both leaf and air temperature are needed. The response
470 of BVOC emissions to temperature discussed here should be interpreted with this potential caveat
471 in mind.

472 While MT emissions remained low and close to the detection limit thus preventing robust
473 quantification of any emission-temperature relationship, isoprene emissions significantly
474 increased with temperature (Fig.9). Figure 9 combines daytime (e.g., with relatively high PAR
475 values) isoprene emission rates from different surface enclosures, with results normalized to
476 account for differing total biomass and species distributions (with *Salix* spp. the dominant emitter).
477 Specifically, we divided all fluxes by the enclosure-specific mean emission at 20 ± 1°C. Emission
478 rates are often standardized to 30°C but we employ 20°C here owing to the colder growth
479 environment at TFS (Ekberg et al., 2009). The isoprene emission-temperature relationship
480 observed at TFS (in blue) is very similar to that reported by Tang et al. (2016) at Abisko (Sweden;
481 in pink) for tundra heath (dominated by evergreen and deciduous dwarf shrubs). Results at TFS
482 and Abisko both point to a high isoprene-temperature response for Arctic ecosystems (Tang et al.,
483 2016). This is further supported by two warming experiments performed in mesic tundra heath
484 (dominated by *Betula nana*, *Empetrum nigrum*, *Empetrum hermaphroditum*, and *Cassiope*
485 *tetragona*) and dry dwarf-shrub tundra (co-dominated by *Empetrum hermaphroditum* and *Salix*
486 *glauca*) in Western Greenland (Kramshøj et al., 2016; Lindwall et al., 2016). Kramshøj et al.
487 (2016) observed a 240% isoprene emission increase with 3°C warming, while Lindwall et al.
488 (2016) reported a 280% increase with 4°C warming. The observationally-derived emission-
489 temperature relationship derived here for TFS reveals a 180-215% emission increase with 3-4°C
490 warming.

491 The MEGAN2.1 modeling framework is commonly used to estimate BVOC fluxes between
492 terrestrial ecosystems and the atmosphere (e.g., Millet et al., 2018). Here, we apply the TFS
493 observations to evaluate the MEGAN2.1 emission-temperature relationship for this Arctic

environment. Figure 9 shows that the model temperature algorithm provides a close fit with observations below 30°C, with a 170-240% emission increase for a 3-4°C warming. While the model predicts a leveling-off of emissions at approximately 30-35°C, our observations reveal no such phenomenon within the 0-40°C enclosure temperature range (Fig. 9). However, given the limited number of enclosure measurements above 30°C, a leveling-off of emissions cannot be statistically ruled out. The key result here is that MEGAN2.1 adequately reproduces the temperature dependence response of Arctic ecosystems in the 0-30°C temperature range – ambient temperature > 30°C being unlikely. The highest air temperature on record at TFS (1988-2019) is 26.5°C, and the mean summertime (June-August) temperature over that period is 9°C. Additionally, for each year in the 1988-2019 historical dataset, there were only 1 to 23 days (0 to 4 days) per year with a maximum temperature above 20°C (above 25°C). If global greenhouse gas emissions continue to increase, temperatures are expected to rise 6-7°C in northern Alaska by the end of the century (annual average; Markon et al., 2012) while the number of days with temperatures above 25°C could triple (Lader et al., 2017). Based on current climate conditions and this rate of change, the MEGAN2.1 algorithm adequately represents the temperature dependence response of Arctic ecosystems for the near and intermediate-term future.

4.2 Long-term effects of warming

BVOC produced by plants are involved in plant growth, reproduction, and defense, and plants use isoprene emissions as a thermotolerance mechanism (Peñuelas and Staudt, 2010; Sasaki et al., 2007). The exponential response of isoprene emissions to temperature observed at TFS adds to a growing body of evidence indicating a high isoprene-temperature response in Arctic ecosystems. However, observations at TFS do not necessarily reflect long-term effects of warming. Schollert et al., (2015) examined how long-term warming affects leaf anatomy of individual arctic plant shoots (*Betula nana*, *Cassiope tetragona*, *Empetrum hermaphroditum*, and *Salix arctica*). They found that long-term warming results in significantly thicker leaves suggesting anatomical acclimation. While the authors hypothesized that this anatomical acclimation may limit the increase of BVOC emissions at plant shoot-level, Kramshøj et al. (2016) later showed that BVOC emissions from Arctic tundra exposed to six years of experimental warming increase at both the plant shoot and ecosystem levels.

In addition to the direct impact of long-term warming on BVOC emissions, ecosystem-level emissions are expected to increase in the Arctic due to climate-driven changes in plant biomass and vegetation composition. For instance, the widespread increase in shrub abundance in the Arctic – due to a longer growing season and enhanced nutrient availability (Berner et al., 2018; Sturm et al., 2001) – will likely significantly affect the BVOC emission potential of the Arctic tundra. Additionally, as mentioned above and as discussed extensively by Peñuelas and Staudt (2010) and Loreto and Schnitlzer (2010), emissions of BVOCs might be largely beneficial for plants, conferring them higher protection from abiotic stressors which are predicted to be more severe in the future. Long-term arctic warming may thus favor BVOC-emitting species even further.

5. Conclusion

While BVOC ambient concentrations and emission rates have been frequently measured in boreal ecosystems, Arctic tundra environments are under studied. We provide here summertime BVOC ambient air mixing ratios and emission rates at Toolik Field Station, on the north flank of the Brooks Range in northern Alaska. We present the first continuous summertime record of ambient air isoprene and its first-generation oxidation products in the Arctic tundra environment. This dataset provides a new set of observations to constrain isoprene chemistry in low-NO_x environments. This dataset also provides a baseline to investigate future changes in the BVOC emission potential of the Arctic tundra environment. While the overall mean isoprene emission rate amounted to 85 $\mu gC/m^2/h$, elevated (> 500 $\mu gC/m^2/h$) isoprene surface emission rates were observed for *Salix* spp., a known isoprene emitter. We also show that the reponse to temperature of isoprene emissions in enclosures dominated by *Salix* spp. increased exponentially in the 0-40°C range, likely conferring greater thermal protection for these plants. Given the widespread increase in shrub abundance in the Arctic (including *Salix* spp.), our results support earlier studies (e.g., Valolahti et al., 2015) suggesting that climate-induced changes in the Arctic vegetation composition will significantly affect the BVOC emission potential of the Arctic tundra, with implications for atmospheric oxidation processes and climate feedbacks.

Data availability

Data are available upon request to the corresponding author.

Author contribution

DH, LH, and DBM designed the experiments and acquired funding. HA led the two field campaigns with significant on-site contribution from KM, JH, LH, DBM, KC, JM, CW, TM, and DH. JH designed and built most of the instruments used in this study. CW acquired the PTR-ToF-MS data during the second campaign and DK performed data analysis. MSBH identified the plant species and provided guidance during the field campaigns. KM and HA analyzed the samples in the lab. HA analyzed all the data and prepared the manuscript with contributions from all co-authors.

Competing interests

The authors declare no competing interests.

Acknowledgements

The authors would like to thank CH2MHill Polar Services for logistical support, the Toolik Field Station staff for assistance with the measurements, and Ilann Bourgeois and Georgios Gkatzelis for helpful discussions. The authors also appreciate the help of Anssi Liikanen who offered kind assistance collecting BVOC samples with the tethered balloon and Wade Permar who helped with PTR-ToF-MS measurements. Finally, the authors gratefully acknowledge Claudia Czimczik and Shawn Pedron at the University of California Irvine for letting us use their soil chamber collars. This research was funded by the National Science Foundation grant #1707569. Undergraduate students Katelyn McErlean, Jacob Moss, and Kaixin Cui received financial support from the University of Colorado Boulder's Undergraduate Research Opportunities Program (UROP; reference #5352323, #4422751, and #4332562, respectively).

References

Akagi, S. K., Yokelson, R. J., Wiedinmyer, C., Alvarado, M. J., Reid, J. S., Karl, T., Crounse, J. D. and Wennberg, P. O.: Emission factors for open and domestic biomass burning for use in atmospheric models, Atmospheric Chem. Phys., 11(9), 4039–4072, doi:https://doi.org/10.5194/acp-11-4039-2011, 2011.

Apel, E. C., Riemer, D. D., Hills, A., Baugh, W., Orlando, J., Faloona, I., Tan, D., Brune, W., Lamb, B., Westberg, H., Carroll, M. A., Thornberry, T. and Geron, C. D.: Measurement and interpretation of isoprene fluxes and isoprene, methacrolein, and methyl vinyl ketone mixing ratios at the PROPHET site during the 1998 Intensive, J. Geophys. Res. Atmospheres, 107(D3), ACH 7-1-ACH 7-15, doi:10.1029/2000JD000225, 2002.

Arneth, A., Harrison, S. P., Zaehle, S., Tsigaridis, K., Menon, S., Bartlein, P. J., Feichter, J., Korhola, A., Kulmala, M., O'Donnell, D., Schurgers, G., Sorvari, S. and Vesala, T.: Terrestrial biogeochemical feedbacks in the climate system, Nat. Geosci., 3(8), 525–532, doi:10.1038/ngeo905, 2010.

Atkinson, R.: Atmospheric chemistry of VOCs and NOx, Atmos. Environ., 34(12), 2063–2101, doi:10.1016/S1352-2310(99)00460-4, 2000.

Bakwin, P. S., Wofsy, S. C., Fan, S.-M. and Fitzjarrald, D. R.: Measurements of NO x and NO y concentrations and fluxes over Arctic tundra, J. Geophys. Res. Atmospheres, 97(D15), 16545–16557, doi:10.1029/91JD00929, 1992.

Bates, K. H. and Jacob, D. J.: A new model mechanism for atmospheric oxidation of isoprene: global effects on oxidants, nitrogen oxides, organic products, and secondary organic aerosol, Atmospheric Chem. Phys., 19(14), 9613–9640, doi:https://doi.org/10.5194/acp-19-9613-2019, 2019.

Berner, L. T., Jantz, P., Tape, K. D. and Goetz, S. J.: Tundra plant above-ground biomass and shrub dominance mapped across the North Slope of Alaska, Environ. Res. Lett., 13(3), 035002, doi:10.1088/1748-9326/aaaa9a, 2018.

Biesenthal, T. A. and Shepson, P. B.: Observations of anthropogenic inputs of the isoprene oxidation products methyl vinyl ketone and methacrolein to the atmosphere, Geophys. Res. Lett., 24(11), 1375–1378, doi:10.1029/97GL01337, 1997.

Biesenthal, T. A., Wu, Q., Shepson, P. B., Wiebe, H. A., Anlauf, K. G. and Mackay, G. I.: A study of relationships between isoprene, its oxidation products, and ozone, in the Lower Fraser Valley, BC - ScienceDirect, Atmospheric Environment, 31(14), 2049–2058, 1997.

Carlton, A. G., Wiedinmyer, C. and Kroll, J. H.: A review of Secondary Organic Aerosol (SOA) formation from isoprene, Atmospheric Chem. Phys., 9(14), 4987–5005, doi:https://doi.org/10.5194/acp-9-4987-2009, 2009.

Dobricic, S., Russo, S., Pozzoli, L., Wilson, J. and Vignati, E.: Increasing occurrence of heat waves in the terrestrial Arctic, Environ. Res. Lett., 15(2), 024022, doi:10.1088/1748-9326/ab6398, 2020.

609 Dunne, E., Galbally, I. E., Cheng, M., Selleck, P., Molloy, S. B. and Lawson, S. J.: Comparison
610 of VOC measurements made by PTR-MS, adsorbent tubes–GC-FID-MS and DNPH
611 derivatization–HPLC during the Sydney Particle Study, 2012: a contribution to the assessment of
612 uncertainty in routine atmospheric VOC measurements, Atmospheric Meas. Tech., 11(1), 141–
613 159, doi:https://doi.org/10.5194/amt-11-141-2018, 2018.

614 Earth Observatory: Arctic Fires Fill the Skies with Soot, [online] Available from:
615 https://earthobservatory.nasa.gov/images/145380/arctic-fires-fill-the-skies-with-
616 soot#targetText=In%20June%20and%20July%202019,harmful%20particles%20into%20the%20
617 air. (Accessed 16 October 2019), 2019.

618 Ekberg, A., Arneth, A., Hakola, H., Hayward, S. and Holst, T.: Isoprene emission from wetland
619 sedges, Biogeosciences, 6(4), 601–613, doi:10.5194/bg-6-601-2009, 2009.

620 Ekberg, A., Arneth, A. and Holst, T.: Isoprene emission from Sphagnum species occupying
621 different growth positions above the water table, Boreal Environ. Res. Int. Interdiscip. J., 16(1),
622 47–59, 2011.

623 Elmendorf, S. C., Henry, G. H. R., Hollister, R. D., Björk, R. G., Boulanger-Lapointe, N., Cooper,
624 E. J., Cornelissen, J. H. C., Day, T. A., Dorrepaal, E., Elumeeva, T. G., Gill, M., Gould, W. A.,
625 Harte, J., Hik, D. S., Hofgaard, A., Johnson, D. R., Johnstone, J. F., Jónsdóttir, I. S., Jorgenson, J.
626 C., Klanderud, K., Klein, J. A., Koh, S., Kudo, G., Lara, M., Lévesque, E., Magnússon, B., May,
627 J. L., Mercado-Dı´az, J. A., Michelsen, A., Molau, U., Myers-Smith, I. H., Oberbauer, S. F.,
628 Onipchenko, V. G., Rixen, C., Schmidt, N. M., Shaver, G. R., Spasojevic, M. J., Þórhallsdóttir, Þ.
629 E., Tolvanen, A., Troxler, T., Tweedie, C. E., Villareal, S., Wahren, C.-H., Walker, X., Webber,
630 P. J., Welker, J. M. and Wipf, S.: Plot-scale evidence of tundra vegetation change and links to
631 recent summer warming, Nat. Clim. Change, 2(6), 453–457, doi:10.1038/nclimate1465, 2012.

632 Faiola, C. L., Erickson, M. H., Fricaud, V. L., Jobson, B. T. and VanReken, T. M.
633 (orcid:0000000226454911): Quantification of biogenic volatile organic compounds with a flame
634 ionization detector using the effective carbon number concept, Atmospheric Meas. Tech. Online,
635 5(8), doi:10.5194/amt-5-1911-2012, 2012.

636 Fares, S., Schnitzhofer, R., Jiang, X., Guenther, A., Hansel, A. and Loreto, F.: Observations of
637 Diurnal to Weekly Variations of Monoterpene-Dominated Fluxes of Volatile Organic Compounds
638 from Mediterranean Forests: Implications for Regional Modeling, Environ. Sci. Technol., 47(19),
639 11073–11082, doi:10.1021/es4022156, 2013.

640 Faubert, P., Tiiva, P., Rinnan, Å., Michelsen, A., Holopainen, J. K. and Rinnan, R.: Doubled
641 volatile organic compound emissions from subarctic tundra under simulated climate warming,
642 New Phytol., 187(1), 199–208, doi:10.1111/j.1469-8137.2010.03270.x, 2010.

643 Fehsenfeld, F., Calvert, J., Fall, R., Goldan, P., Guenther, A. B., Hewitt, C. N., Lamb, B., Liu, S.,
644 Trainer, M., Westberg, H. and Zimmerman, P.: Emissions of volatile organic compounds from
645 vegetation and the implications for atmospheric chemistry, Glob. Biogeochem. Cycles, 6(4), 389–
646 430, doi:10.1029/92GB02125, 1992.

Fontijn, Arthur., Sabadell, A. J. and Ronco, R. J.: Homogeneous chemiluminescent measurement of nitric oxide with ozone. Implications for continuous selective monitoring of gaseous air pollutants, Anal. Chem., 42(6), 575–579, doi:10.1021/ac60288a034, 1970.

Forbes, B. C., Fauria, M. M. and Zetterberg, P.: Russian Arctic warming and 'greening' are closely tracked by tundra shrub willows, Glob. Change Biol., 16(5), 1542–1554, doi:10.1111/j.1365-2486.2009.02047.x, 2010.

Freedman, A. and Cappucci, M.: Parts of Siberia are hotter than Washington, with temperatures nearly 40 degrees above average, Wash. Post, 22nd May [online] Available from: https://www.washingtonpost.com/weather/2020/05/22/siberia-heat-wave/ (Accessed 29 May 2020), 2020.

Fuentes, J. D., Lerdau, M., Atkinson, R., Baldocchi, D., Bottenheim, J. W., Ciccioli, P., Lamb, B., Geron, C., Gu, L., Guenther, A., Sharkey, T. D. and Stockwell, W.: Biogenic Hydrocarbons in the Atmospheric Boundary Layer: A Review, Bull. Am. Meteorol. Soc., 81(7), 1537–1576, doi:10.1175/1520-0477(2000)081<1537:BHITAB>2.3.CO;2, 2000.

Gough, L.: Relative percent cover of plant species for years 2012-2017 in the Arctic Long-term Ecological Research (ARC-LTER) 1989 moist acidic tundra (MAT89) experimental plots, Toolik Field Station, Alaska., , doi:10.6073/PASTA/F31DEF760DB3F8E6CFEE5FEE07CC693E, 2019.

de Gouw, J. A., Goldan, P. D., Warneke, C., Kuster, W. C., Roberts, J. M., Marchewka, M., Bertman, S. B., Pszenny, A. a. P. and Keene, W. C.: Validation of proton transfer reaction-mass spectrometry (PTR-MS) measurements of gas-phase organic compounds in the atmosphere during the New England Air Quality Study (NEAQS) in 2002, J. Geophys. Res. Atmospheres, 108(D21), doi:10.1029/2003JD003863, 2003.

Guenther, A., Hewitt, C. N., Erickson, D., Fall, R., Geron, C., Graedel, T., Harley, P., Klinger, L., Lerdau, M., Mckay, W. A., Pierce, T., Scholes, B., Steinbrecher, R., Tallamraju, R., Taylor, J. and Zimmerman, P.: A global model of natural volatile organic compound emissions, J. Geophys. Res. Atmospheres, 100(D5), 8873–8892, doi:10.1029/94JD02950, 1995.

Guenther, A., Karl, T., Harley, P., Wiedinmyer, C., Palmer, P. I. and Geron, C.: Estimates of global terrestrial isoprene emissions using MEGAN (Model of Emissions of Gases and Aerosols from Nature), Atmospheric Chem. Phys., 6(11), 3181–3210, doi:https://doi.org/10.5194/acp-6-3181-2006, 2006.

Guenther, A. B., Zimmerman, P. R., Harley, P. C., Monson, R. K. and Fall, R.: Isoprene and monoterpene emission rate variability: Model evaluations and sensitivity analyses, J. Geophys. Res. Atmospheres, 98(D7), 12609–12617, doi:10.1029/93JD00527, 1993.

Guenther, A. B., Jiang, X., Heald, C. L., Sakulyanontvittaya, T., Duhl, T., Emmons, L. K. and Wang, X.: The Model of Emissions of Gases and Aerosols from Nature version 2.1 (MEGAN2.1): an extended and updated framework for modeling biogenic emissions, Geosci. Model Dev., 5(6), 1471–1492, doi:https://doi.org/10.5194/gmd-5-1471-2012, 2012.

Hakola, H., Laurila, T., Rinne, J. and Puhto, K.: The ambient concentrations of biogenic hydrocarbons at a northern European, boreal site, Atmos. Environ., 34(29), 4971–4982, doi:10.1016/S1352-2310(00)00192-8, 2000.

Hakola, H., Tarvainen, V., Laurila, T., Hiltunen, V., Hellén, H. and Keronen, P.: Seasonal variation of VOC concentrations above a boreal coniferous forest, Atmos. Environ., 37(12), 1623–1634, doi:10.1016/S1352-2310(03)00014-1, 2003.

Helmig, D.: Ozone removal techniques in the sampling of atmospheric volatile organic trace gases, Atmos. Environ., 31(21), 3635–3651, doi:10.1016/S1352-2310(97)00144-1, 1997.

Helmig, D., Balsley, B., Davis, K., Kuck, L. R., Jensen, M., Bognar, J., Smith, T., Arrieta, R. V., Rodríguez, R. and Birks, J. W.: Vertical profiling and determination of landscape fluxes of biogenic nonmethane hydrocarbons within the planetary boundary layer in the Peruvian Amazon, J. Geophys. Res. Atmospheres, 103(D19), 25519–25532, doi:10.1029/98JD01023, 1998.

Helmig, D., Bocquet, F., Pollmann, J. and Revermann, T.: Analytical techniques for sesquiterpene emission rate studies in vegetation enclosure experiments, Atmos. Environ., 38(4), 557–572, doi:10.1016/j.atmosenv.2003.10.012, 2004.

Hollesen, J., Buchwal, A., Rachlewicz, G., Hansen, B. U., Hansen, M. O., Stecher, O. and Elberling, B.: Winter warming as an important co-driver for Betula nana growth in western Greenland during the past century, in Global change biology., 2015.

Holst, T., Arneth, A., Hayward, S., Ekberg, A., Mastepanov, M., Jackowicz-Korczynski, M., Friborg, T., Crill, P. M. and Bäckstrand, K.: BVOC ecosystem flux measurements at a high latitude wetland site, Atmospheric Chem. Phys., 10(4), 1617–1634, doi:https://doi.org/10.5194/acp-10-1617-2010, 2010.

Holton, J. R. and Hakim, G. J.: Chapter 8 - The Planetary Boundary Layer, in An Introduction to Dynamic Meteorology (Fifth Edition), edited by J. R. Holton and G. J. Hakim, pp. 255–277, Academic Press, Boston., 2013.

Honrath, R. E. and Jaffe, D. A.: The seasonal cycle of nitrogen oxides in the Arctic troposphere at Barrow, Alaska, J. Geophys. Res. Atmospheres, 97(D18), 20615–20630, doi:10.1029/92JD02081, 1992.

Hu, L., Millet, D. B., Baasandorj, M., Griffis, T. J., Turner, P., Helmig, D., Curtis, A. J. and Hueber, J.: Isoprene emissions and impacts over an ecological transition region in the U.S. Upper Midwest inferred from tall tower measurements, J. Geophys. Res. Atmospheres, 120(8), 3553–3571, doi:10.1002/2014JD022732, 2015.

Isaacman-VanWertz, G., Sueper, D. T., Aikin, K. C., Lerner, B. M., Gilman, J. B., de Gouw, J. A., Worsnop, D. R. and Goldstein, A. H.: Automated single-ion peak fitting as an efficient approach for analyzing complex chromatographic data, J. Chromatogr. A, 1529, 81–92, doi:10.1016/j.chroma.2017.11.005, 2017.

720 Jardine, K. J., Monson, R. K., Abrell, L., Saleska, S. R., Arneth, A., Jardine, A., Ishida, F. Y.,
721 Serrano, A. M. Y., Artaxo, P., Karl, T., Fares, S., Goldstein, A., Loreto, F. and Huxman, T.:
722 Within-plant isoprene oxidation confirmed by direct emissions of oxidation products methyl vinyl
723 ketone and methacrolein, Glob. Change Biol., 18(3), 973–984, doi:10.1111/j.1365-
724 2486.2011.02610.x, 2012.

725 Kade, A., Bret-Harte, M. S., Euskirchen, E. S., Edgar, C. and Fulweber, R. A.: Upscaling of CO2
726 fluxes from heterogeneous tundra plant communities in Arctic Alaska, J. Geophys. Res.
727 Biogeosciences, 117(G4), doi:10.1029/2012JG002065, 2012.

728 Karbiwnyk, C. M., Mills, C. S., Helmig, D. and Birks, J. W.: Minimization of water vapor
729 interference in the analysis of non-methane volatile organic compounds by solid adsorbent
730 sampling, J. Chromatogr. A, 958(1–2), 219–229, doi:10.1016/s0021-9673(02)00307-2, 2002.

731 Karbiwnyk, C. M., Mills, C. S., Helmig, D. and Birks, J. W.: Use of chloroflurocarbons as internal
732 standards for the measurement of atmospheric non-methane volatile organic compounds sampled
733 onto solid adsorbent cartridges, Environ. Sci. Technol., 37(5), 1002–1007,
734 doi:10.1021/es025910q, 2003.

735 Karl, T., Potosnak, M., Guenther, A., Clark, D., Walker, J., Herrick, J. D. and Geron, C.: Exchange
736 processes of volatile organic compounds above a tropical rain forest: Implications for modeling
737 tropospheric chemistry above dense vegetation, J. Geophys. Res. Atmospheres, 109(D18),
738 doi:10.1029/2004JD004738, 2004.

739 Kramshøj, M., Vedel-Petersen, I., Schollert, M., Rinnan, Å., Nymand, J., Ro-Poulsen, H. and
740 Rinnan, R.: Large increases in Arctic biogenic volatile emissions are a direct effect of warming,
741 Nat. Geosci., 9(5), 349–352, doi:10.1038/ngeo2692, 2016.

742 Kulmala, M., Suni, T., Lehtinen, K. E. J., Maso, M. D., Boy, M., Reissell, A., Rannik, Ü., Aalto,
743 P., Keronen, P., Hakola, H., Bäck, J., Hoffmann, T., Vesala, T. and Hari, P.: A new feedback
744 mechanism linking forests, aerosols, and climate, Atmospheric Chem. Phys., 4(2), 557–562,
745 doi:https://doi.org/10.5194/acp-4-557-2004, 2004.

746 Lader, R., Walsh, J. E., Bhatt, U. S. and Bieniek, P. A.: Projections of Twenty-First-Century
747 Climate Extremes for Alaska via Dynamical Downscaling and Quantile Mapping, J. Appl.
748 Meteorol. Climatol., 56(9), 2393–2409, doi:10.1175/JAMC-D-16-0415.1, 2017.

749 Lappalainen, H. K., Sevanto, S., Bäck, J., Ruuskanen, T. M., Kolari, P., Taipale, R., Rinne, J.,
750 Kulmala, M. and Hari, P.: Day-time concentrations of biogenic volatile organic compounds in a
751 boreal forest canopy and their relation to environmental and biological factors, Atmospheric
752 Chem. Phys., 9(15), 5447–5459, doi:https://doi.org/10.5194/acp-9-5447-2009, 2009.

753 Li, T., Holst, T., Michelsen, A. and Rinnan, R.: Amplification of plant volatile defence against
754 insect herbivory in a warming Arctic tundra, Nat. Plants, 5(6), 568–574, doi:10.1038/s41477-019-
755 0439-3, 2019.

Lim, H.-J., Carlton, A. G. and Turpin, B. J.: Isoprene Forms Secondary Organic Aerosol through Cloud Processing: Model Simulations, Environ. Sci. Technol., 39(12), 4441–4446, doi:10.1021/es048039h, 2005.

Lindfors, V., Laurila, T., Hakola, H., Steinbrecher, R. and Rinne, J.: Modeling speciated terpenoid emissions from the European boreal forest, Atmos. Environ., 34(29), 4983–4996, doi:10.1016/S1352-2310(00)00223-5, 2000.

Lindwall, F., Faubert, P. and Rinnan, R.: Diel Variation of Biogenic Volatile Organic Compound Emissions- A field Study in the Sub, Low and High Arctic on the Effect of Temperature and Light, PLOS ONE, 10(4), e0123610, doi:10.1371/journal.pone.0123610, 2015.

Lindwall, F., Schollert, M., Michelsen, A., Blok, D. and Rinnan, R.: Fourfold higher tundra volatile emissions due to arctic summer warming, J. Geophys. Res. Biogeosciences, 121(3), 895–902, doi:10.1002/2015JG003295, 2016.

Liu, X., Pawliszyn, R., Wang, L. and Pawliszyn, J.: On-site monitoring of biogenic emissions from Eucalyptus dunnii leaves using membrane extraction with sorbent interface combined with a portable gas chromatograph system, The Analyst, 129(1), 55–62, doi:10.1039/b311998j, 2004.

Loreto, F. and Schnitzler, J.-P.: Abiotic stresses and induced BVOCs, Trends Plant Sci., 15(3), 154–166, doi:10.1016/j.tplants.2009.12.006, 2010.

Macias-Fauria, M., Forbes, B. C., Zetterberg, P. and Kumpula, T.: Eurasian Arctic greening reveals teleconnections and the potential for structurally novel ecosystems, Nat. Clim. Change, 2(8), 613–618, doi:10.1038/nclimate1558, 2012.

Markon, C. J., Trainor, S. F. and Chapin, F. S.: The United States National Climate Assessment - Alaska Technical Regional Report. [online] Available from: https://pubs.usgs.gov/circ/1379/pdf/circ1379.pdf, 2012.

Michelsen, A., Rinnan, R. and Jonasson, S.: Two decades of experimental manipulations of heaths and forest understory in the subarctic, Ambio, 41 Suppl 3, 218–230, doi:10.1007/s13280-012-0303-4, 2012.

Millet, D. B., Alwe, H. D., Chen, X., Deventer, M. J., Griffis, T. J., Holzinger, R., Bertman, S. B., Rickly, P. S., Stevens, P. S., Léonardis, T., Locoge, N., Dusanter, S., Tyndall, G. S., Alvarez, S. L., Erickson, M. H. and Flynn, J. H.: Bidirectional Ecosystem–Atmosphere Fluxes of Volatile Organic Compounds Across the Mass Spectrum: How Many Matter?, ACS Earth Space Chem., doi:10.1021/acsearthspacechem.8b00061, 2018.

Olofsson, M., Ek-Olausson, B., Jensen, N. O., Langer, S. and Ljungström, E.: The flux of isoprene from a willow coppice plantation and the effect on local air quality, Atmos. Environ., 39(11), 2061–2070, doi:10.1016/j.atmosenv.2004.12.015, 2005.

Ormeño, E., Mevy, J. P., Vila, B., Bousquet-Melou, A., Greff, S., Bonin, G. and Fernandez, C.: Water deficit stress induces different monoterpene and sesquiterpene emission changes in

792 Mediterranean species. Relationship between terpene emissions and plant water potential.,
793 Chemosphere, 67(2), 276–284, 2007.

794 Ortega, J. and Helmig, D.: Approaches for quantifying reactive and low-volatility biogenic organic
795 compound emissions by vegetation enclosure techniques – Part A, Chemosphere, 72(3), 343–364,
796 doi:10.1016/j.chemosphere.2007.11.020, 2008.

797 Ortega, J., Helmig, D., Daly, R. W., Tanner, D. M., Guenther, A. B. and Herrick, J. D.: Approaches
798 for quantifying reactive and low-volatility biogenic organic compound emissions by vegetation
799 enclosure techniques – Part B: Applications, Chemosphere, 72(3), 365–380,
800 doi:10.1016/j.chemosphere.2008.02.054, 2008.

801 Overland, J. E., Wang, M., Walsh, J. E. and Stroeve, J. C.: Future Arctic climate changes:
802 Adaptation and mitigation time scales, Earths Future, 2(2), 68–74, doi:10.1002/2013EF000162,
803 2014.

804 Peñuelas, J. and Staudt, M.: BVOCs and global change, Trends Plant Sci., 15(3), 133–144,
805 doi:10.1016/j.tplants.2009.12.005, 2010.

806 Pollmann, J., Ortega, J. and Helmig, D.: Analysis of Atmospheric Sesquiterpenes: Sampling
807 Losses and Mitigation of Ozone Interferences, Environ. Sci. Technol., 39(24), 9620–9629,
808 doi:10.1021/es050440w, 2005.

809 Potosnak, M. J., Baker, B. M., LeStourgeon, L., Disher, S. M., Griffin, K. L., Bret-Harte, M. S.
810 and Starr, G.: Isoprene emissions from a tundra ecosystem, Biogeosciences, 10(2), 871–889,
811 doi:10.5194/bg-10-871-2013, 2013.

812 Pressley, S., Lamb, B., Westberg, H., Flaherty, J., Chen, J. and Vogel, C.: Long-term isoprene flux
813 measurements above a northern hardwood forest, J. Geophys. Res. Atmospheres, 110(D7),
814 doi:10.1029/2004JD005523, 2005.

815 Raynolds, M. K., Walker, D. A., Balser, A., Bay, C., Campbell, M., Cherosov, M. M., Daniëls, F.
816 J. A., Eidesen, P. B., Ermokhina, K. A., Frost, G. V., Jedrzejek, B., Jorgenson, M. T., Kennedy,
817 B. E., Kholod, S. S., Lavrinenko, I. A., Lavrinenko, O. V., Magnússon, B., Matveyeva, N. V.,
818 Metúsalemsson, S., Nilsen, L., Olthof, I., Pospelov, I. N., Pospelova, E. B., Pouliot, D., Razzhivin,
819 V., Schaepman-Strub, G., Šibík, J., Telyatnikov, M. Yu. and Troeva, E.: A raster version of the
820 Circumpolar Arctic Vegetation Map (CAVM), Remote Sens. Environ., 232, 111297,
821 doi:10.1016/j.rse.2019.111297, 2019.

822 Rinnan, R., Rinnan, Å., Faubert, P., Tiiva, P., Holopainen, J. K. and Michelsen, A.: Few long-term
823 effects of simulated climate change on volatile organic compound emissions and leaf chemistry of
824 three subarctic dwarf shrubs, Environ. Exp. Bot., 72(3), 377–386,
825 doi:10.1016/j.envexpbot.2010.11.006, 2011.

826 Rinnan, R., Steinke, M., McGenity, T. and Loreto, F.: Plant volatiles in extreme terrestrial and
827 marine environments, Plant Cell Environ., 37(8), 1776–1789, doi:10.1111/pce.12320, 2014.

828 Rinne, H. J. I., Guenther, A. B., Greenberg, J. P. and Harley, P. C.: Isoprene and monoterpene
829 fluxes measured above Amazonian rainforest and their dependence on light and temperature,
830 Atmos. Environ., 36(14), 2421–2426, doi:10.1016/S1352-2310(01)00523-4, 2002.

831 Rinne, J., Bäck, J. and Hakola, H.: Biogenic volatile organic compound emissions from the
832 Eurasian taiga: current knowledge and future directions, , 14, 20, 2009.

833 Rivera-Rios, J. C., Nguyen, T. B., Crounse, J. D., Jud, W., Clair, J. M. S., Mikoviny, T., Gilman,
834 J. B., Lerner, B. M., Kaiser, J. B., Gouw, J. de, Wisthaler, A., Hansel, A., Wennberg, P. O.,
835 Seinfeld, J. H. and Keutsch, F. N.: Conversion of hydroperoxides to carbonyls in field and
836 laboratory instrumentation: Observational bias in diagnosing pristine versus anthropogenically
837 controlled atmospheric chemistry, Geophys. Res. Lett., 41(23), 8645–8651,
838 doi:10.1002/2014GL061919, 2014.

839 Ruuskanen, T. M., Kolari, P., Bäck, J., Kulmala, M., Rinne, J., Hakola, H., Taipale, R., Raivonen,
840 M., Altimir, N. and Hari, P.: On-line field measurements of monoterpene emissions from Scots
841 pine by proton-transfer-reaction mass spectrometry, Boreal Environ. Res., 10(6), 553–567, 2005.

842 Sasaki, K., Saito, T. and Lamsa, M.: Plants utilize isoprene emission as a thermotolerance
843 mechanism, Plant Cell Physiol., 48, 1254–1262, 2007.

844 Scanlon, J. T. and Willis, D. E.: Calculation of Flame Ionization Detector Relative Response
845 Factors Using the Effective Carbon Number Concept, J. Chromatogr. Sci., 23(8), 333–340,
846 doi:10.1093/chromsci/23.8.333, 1985.

847 Schollert, M., Burchard, S., Faubert, P., Michelsen, A. and Rinnan, R.: Biogenic volatile organic
848 compound emissions in four vegetation types in high arctic Greenland, Polar Biol., 37(2), 237–
849 249, doi:10.1007/s00300-013-1427-0, 2014.

850 Schollert, M., Kivimäenpää, M., Valolahti, H. M. and Rinnan, R.: Climate change alters leaf
851 anatomy, but has no effects on volatile emissions from arctic plants, Plant Cell Environ., 38(10),
852 2048–2060, doi:10.1111/pce.12530, 2015.

853 Shaver, G. R. and Chapin, F. S.: Production: Biomass Relationships and Element Cycling in
854 Contrasting Arctic Vegetation Types, Ecol. Monogr., 61(1), 1–31, doi:10.2307/1942997, 1991.

855 Sindelarova, K., Granier, C., Bouarar, I., Guenther, A., Tilmes, S., Stavrakou, T., Müller, J.-F.,
856 Kuhn, U., Stefani, P. and Knorr, W.: Global data set of biogenic VOC emissions calculated by the
857 MEGAN model over the last 30 years, Atmospheric Chem. Phys., 14(17), 9317–9341,
858 doi:https://doi.org/10.5194/acp-14-9317-2014, 2014.

859 Sistla, S. A., Moore, J. C., Simpson, R. T., Gough, L., Shaver, G. R. and Schimel, J. P.: Long-term
860 warming restructures Arctic tundra without changing net soil carbon storage, Nature, 497(7451),
861 615–618, doi:10.1038/nature12129, 2013.

862 Spirig, C., Guenther, A., Greenberg, J. P., Calanca, P. and Tarvainen, V.: Tethered balloon
863 measurements of biogenic volatile organic compounds at a Boreal forest site, Atmospheric Chem.
864 Phys., 4(1), 215–229, doi:https://doi.org/10.5194/acp-4-215-2004, 2004.

865 Sturm, M., Racine, C. and Tape, K.: Climate change: Increasing shrub abundance in the Arctic,
866 Nature, 411(6837), 546–547, doi:10.1038/35079180, 2001.

867 Sullivan, P. F., Sommerkorn, M., Rueth, H. M., Nadelhoffer, K. J., Shaver, G. R. and Welker, J.
868 M.: Climate and species affect fine root production with long-term fertilization in acidic tussock
869 tundra near Toolik Lake, Alaska, Oecologia, 153(3), 643–652, doi:10.1007/s00442-007-0753-8,
870 2007.

871 Survey: Maps - Toolik Lake Area Vegetation, [online] Available from:
872 http://www.arcticatlas.org/maps/themes/tl5k/tl5kvg (Accessed 30 September 2019), 2012.

873 Tang, J., Schurgers, G., Valolahti, H., Faubert, P., Tiiva, P., Michelsen, A. and Rinnan, R.:
874 Challenges in modelling isoprene and monoterpene emission dynamics of Arctic plants: a case
875 study from a subarctic tundra heath, Biogeosciences, 13(24), 6651–6667,
876 doi:https://doi.org/10.5194/bg-13-6651-2016, 2016.

877 Tape, K., Sturm, M. and Racine, C.: The evidence for shrub expansion in Northern Alaska and the
878 Pan-Arctic, Glob. Change Biol., 12(4), 686–702, doi:10.1111/j.1365-2486.2006.01128.x, 2006.

879 Tarvainen, V., Hakola, H., Rinne, J., HellàN, H. and Haapanala, S.: Towards a comprehensive
880 emission inventory of terpenoids from boreal ecosystems, Tellus B Chem. Phys. Meteorol., 59(3),
881 526–534, doi:10.1111/j.1600-0889.2007.00263a.x, 2007.

882 Tiiva, P., Faubert, P., Michelsen, A., Holopainen, T., Holopainen, J. K. and Rinnan, R.: Climatic
883 warming increases isoprene emission from a subarctic heath, New Phytol., 180(4), 853–863,
884 doi:10.1111/j.1469-8137.2008.02587.x, 2008.

885 Toolik Field Station Environmental Data Center: Toolik Field Station::Weather Data Query,
886 [online] Available from: https://toolik.alaska.edu/edc/abiotic_monitoring/data_query.php
887 (Accessed 30 September 2019), 2019.

888 Tsigaridis, K. and Kanakidou, M.: Secondary organic aerosol importance in the future atmosphere,
889 Atmos. Environ., 41(22), 4682–4692, doi:10.1016/j.atmosenv.2007.03.045, 2007.

890 Unger, N.: Human land-use-driven reduction of forest volatiles cools global climate, Nat. Clim.
891 Change, 4(10), 907–910, doi:10.1038/nclimate2347, 2014.

892 Valolahti, H., Kivimäenpää, M., Faubert, P., Michelsen, A. and Rinnan, R.: Climate change-
893 induced vegetation change as a driver of increased subarctic biogenic volatile organic compound
894 emissions, Glob. Change Biol., 21(9), 3478–3488, doi:10.1111/gcb.12953, 2015.

895 Van Dam, B., Helmig, D., Burkhart, J. F., Obrist, D. and Oltmans, S. J.: Springtime boundary layer
896 O3 and GEM depletion at Toolik Lake, Alaska, J. Geophys. Res. Atmospheres, 118(8), 3382–
897 3391, doi:10.1002/jgrd.50213, 2013.

898 Van Dam, B., Helmig, D., Doskey, P. V. and Oltmans, S. J.: Summertime surface O3 behavior
899 and deposition to tundra in the Alaskan Arctic, J. Geophys. Res. Atmospheres, 121(13), 8055–
900 8066, doi:10.1002/2015JD023914, 2016.

Vedel-Petersen, I., Schollert, M., Nymand, J. and Rinnan, R.: Volatile organic compound emission profiles of four common arctic plants, Atmos. Environ., 120, 117–126, doi:10.1016/j.atmosenv.2015.08.082, 2015.

Walker, M. D., Walker, D. A. and Auerbach, N. A.: Plant communities of a tussock tundra landscape in the Brooks Range Foothills, Alaska, J. Veg. Sci., 5(6), 843–866, doi:10.2307/3236198, 1994.

Wang, J.-L., Chew, C., Chen, S.-W. and Kuo, S.-R.: Concentration Variability of Anthropogenic Halocarbons and Applications as Internal Reference in Volatile Organic Compound Measurements, Environ. Sci. Technol., 34(11), 2243–2248, doi:10.1021/es991128n, 2000.

Zini, C. A., Augusto, F., Christensen, T. E., Smith, B. P., Caramão, E. B. and Pawliszy, J.: Monitoring biogenic volatile compounds emitted by Eucalyptus citriodora using SPME, Anal. Chem., 73(19), 4729–4735, doi:10.1021/ac0103219, 2001.

914 Table 1: Year 2017 median relative percent cover of plant species in moist acidic tundra long-term
915 ecological research (LTER) experimental control plots at Toolik Field Station. The last column indicates
916 whether plant species were present in surface or bag enclosure experiments in this study.

Plant name	Relative land surface cover in moist acidic tundra (%) (Gough, 2019)	Present in surface or bag enclosures
Andromeda polifolia	0.6	yes
Betula nana	14.4	yes
Carex bigelowii	1.0	yes
Cassiope tetragona	2.0	yes
Empetrum nigrum	3.8	yes
Eriophorum vaginatum	8.6	yes
Ledum palustre	10.5	yes
Mixed Lichens	2.1	yes
Mixed moss	6.0	yes
Pedicularis lapponica	0.6	no
Polygonum bistorta	0.6	no
Rubus chamaemorus	20.2	no
Salix pulchra	4.9	yes
Vaccinium uliginosum	1.9	yes
Vaccinium vitis-idaea	6.6	yes

917

918

919

920

921

Table 2: Average mixings ratios with standard deviation, along with minimum (min) and maximum (max) values and quantification frequency (QF) of the measured monoterpenes in ambient air. LOQ stands for limit of quantification. For values lower than the LOQ, mixing ratios equal to half of the LOQ were used to calculate the mean.

	mean ± standard deviation (pptv)	Min (pptv)	Max (pptv)	QF (%)
α-pinene	11.7 ± 8.1	< LOQ	61.6	88
camphene	< LOQ	< LOQ	21.9	11
sabinene	< LOQ	< LOQ	34.2	11
p-cymene	2.0 ± 1.9	< LOQ	12.3	32
limonene	< LOQ	< LOQ	2.9	< 1

Table 3: Isoprene and monoterpenes (sum of α-pinene, β-pinene, limonene, and 1,8-cineole) surface emission rates per vegetation type. Miscellaneous refers to a mix of different species, including lichens and moss tundra (see Fig.S.I.3-15). Daytime refers to 10 am-8 pm, midday to 11 am-2 pm, and nighttime to 11 pm-5 am (Alaska Standard Time). The values in brackets represent the average enclosure temperature for each emission rate.

	mean ± standard deviation ($\mu gC/m^2/h$)	daytime mean ± standard deviation ($\mu gC/m^2/h$)	midday mean ± standard deviation ($\mu gC/m^2/h$)	nighttime mean ± standard deviation ($\mu gC/m^2/h$)
isoprene				
Salix spp.	149 ± 327 [17.6°C]	232 ± 400 [23.9°C]	334 ± 473 [27.0°C]	7 ± 10 [8.0°C]
Betula spp.	12 ± 30 [13.7°C]	19 ± 38 [17.4°C]	28 ± 37 [20.1°C]	5 ± 14 [5.8°C]
Miscellaneous	38 ± 81 [11.8°C]	57 ± 100 [14.8°C]	104 ± 135 [16.2°C]	21 ± 64 [8.2°C]
monoterpenes				
Salix spp.	0.8 ± 1.3 [17.6°C]	1.1 ± 1.5 [23.9°C]	1.4 ± 1.7 [27.0°C]	0.4 ± 1.0 [8.0°C]
Betula spp.	0.5 ± 0.6 [13.7°C]	0.7 ± 0.7 [17.4°C]	1.0 ± 0.8 [20.1°C]	0.2 ± 0.2 [5.8°C]
Miscellaneous	1.1 ± 1.4 [11.8°C]	1.3 ± 1.6 [14.8°C]	1.7 ± 2.0 [16.2°C]	1.0 ± 1.4 [8.2°C]

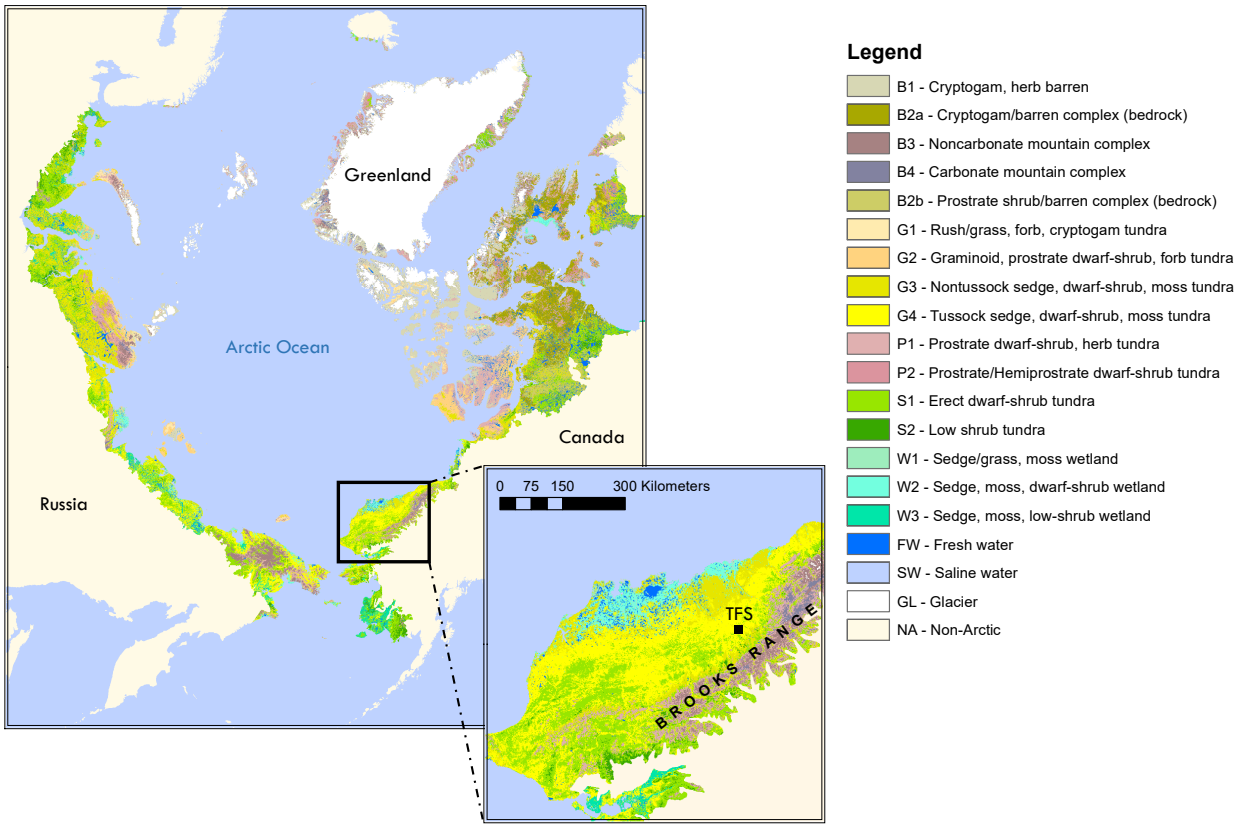

Figure 1: Location of Toolik Field Station (TFS) on the north flanks of the Brooks Range in northern Alaska along with arctic vegetation type. This Figure was made using the raster version of the Circumpolar Arctic Vegetation Map prepared by Raynolds et al. (2019) and publicly available at www.geobotany.uaf.edu.

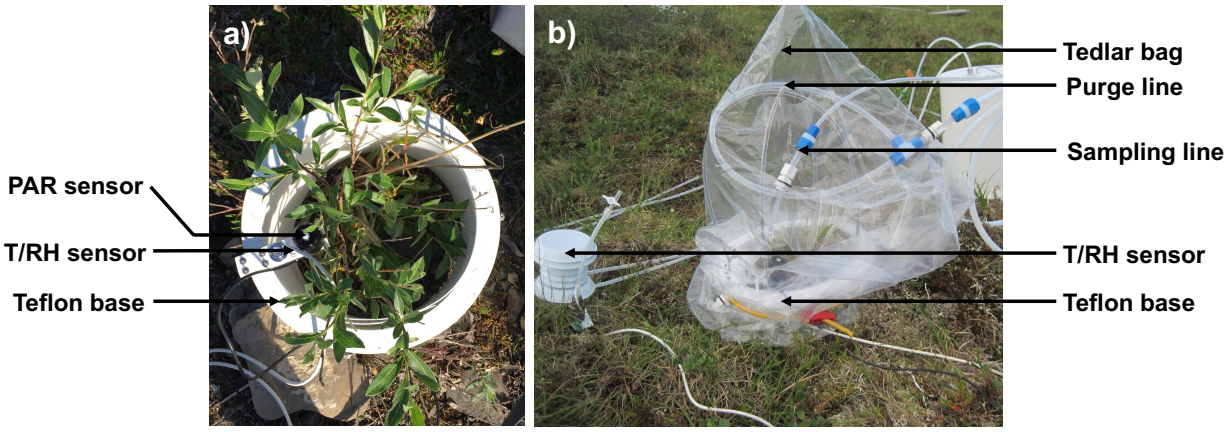

965

966 Figure 2: Photographs of a surface enclosure experiment setup at Toolik Field Station, Alaska. a) The first
967 step of the installation consisted in positioning the Teflon® base around the vegetation of interest along
968 with temperature (T), relative humidity (RH), and photosynthetically active radiation (PAR) sensors. b)
969 The second step consisted in positioning the Tedlar® bag around the base. The bag was connected to a
970 purge air and a sampling line. An additional T/RH sensor was also positioned outside the bag.

971

972

973

974

975

976

977

978

979

980

981

982

983

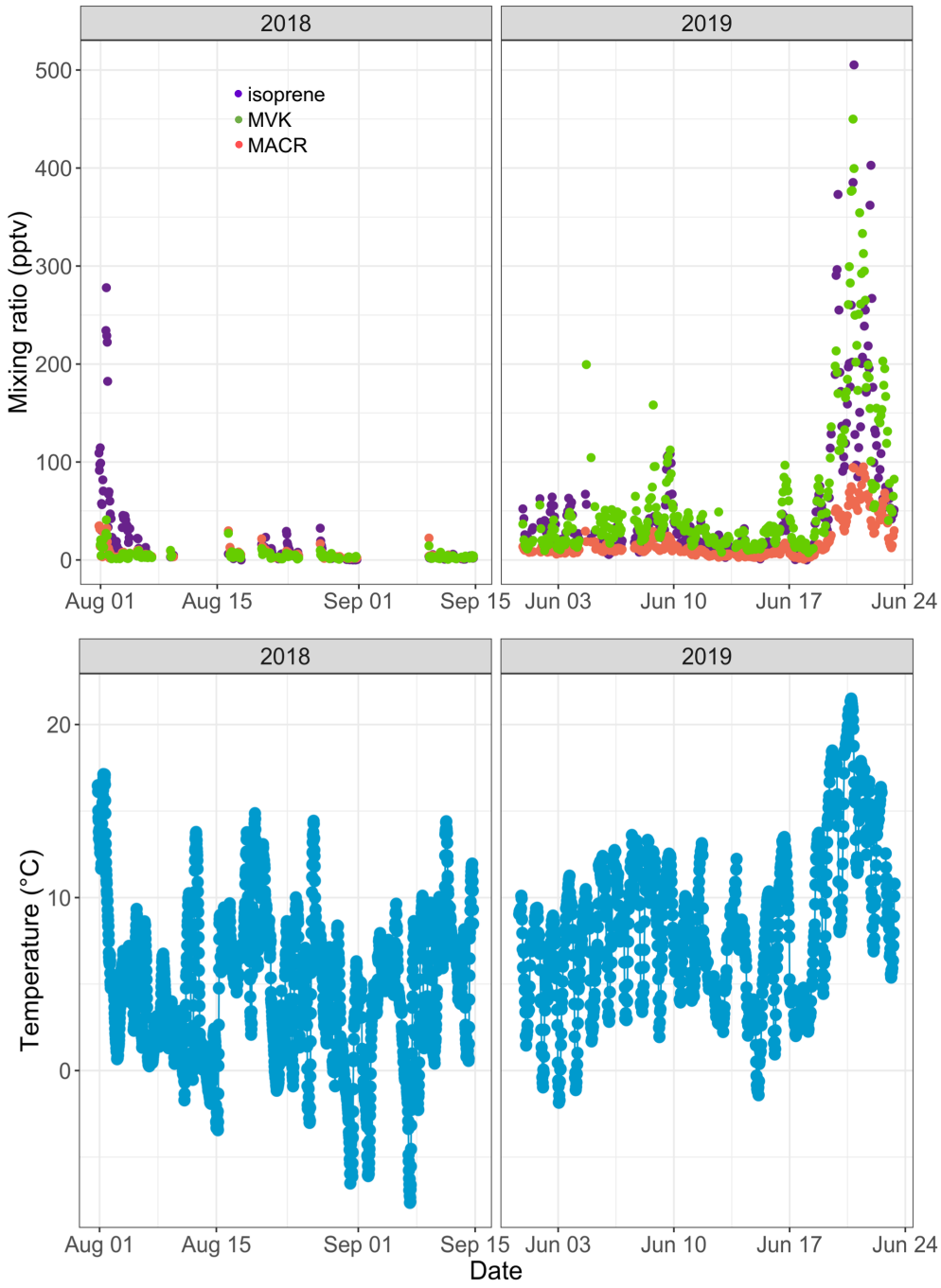

984

985 Figure 3: Time-series of isoprene (purple), methylvinylketone (MVK, green), and methacrolein (MACR,
986 salmon) mixing ratios (in pptv) in ambient air at Toolik Field station (top panels) and of 30-min-averaged
987 ambient temperature (in °C) at 4 meters above ground level (bottom panels).

988

989

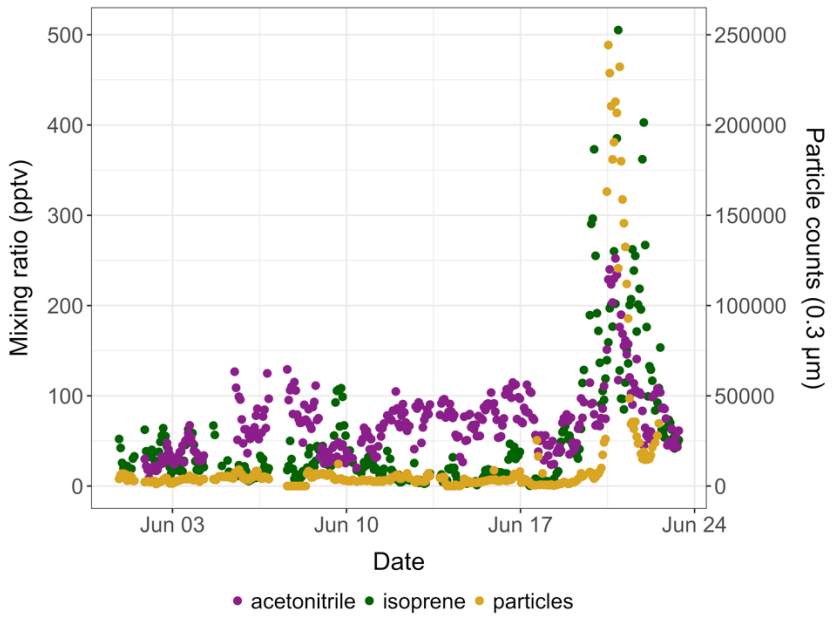

990

991 Figure 4: Time-series of isoprene (green) and acetonitrile (purple) mixing ratios (in pptv) and of 0.3 µm
992 particle counts (yellow) in ambient air at Toolik Field station in June 2019.

993

994

995

996

997

998

999

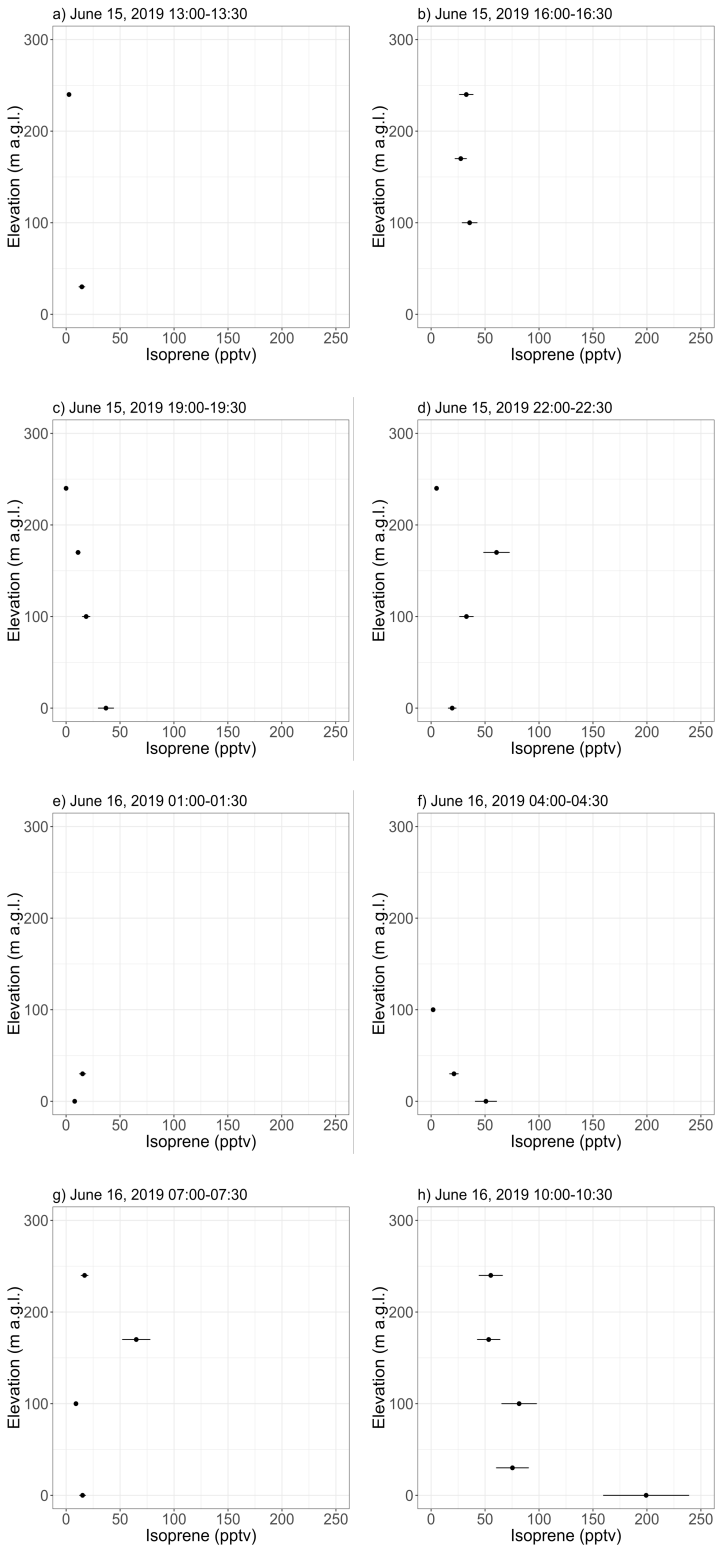

Figure 5: Vertical profiles of isoprene mixing ratios as inferred from 30-min samples collected with a tethered balloon. The error bars show the analytical uncertainty for isoprene (20 %). Samples with an isoprene mixing ratio lower than blanks were discarded. Hours are in Alaska Standard Time (UTC-9).

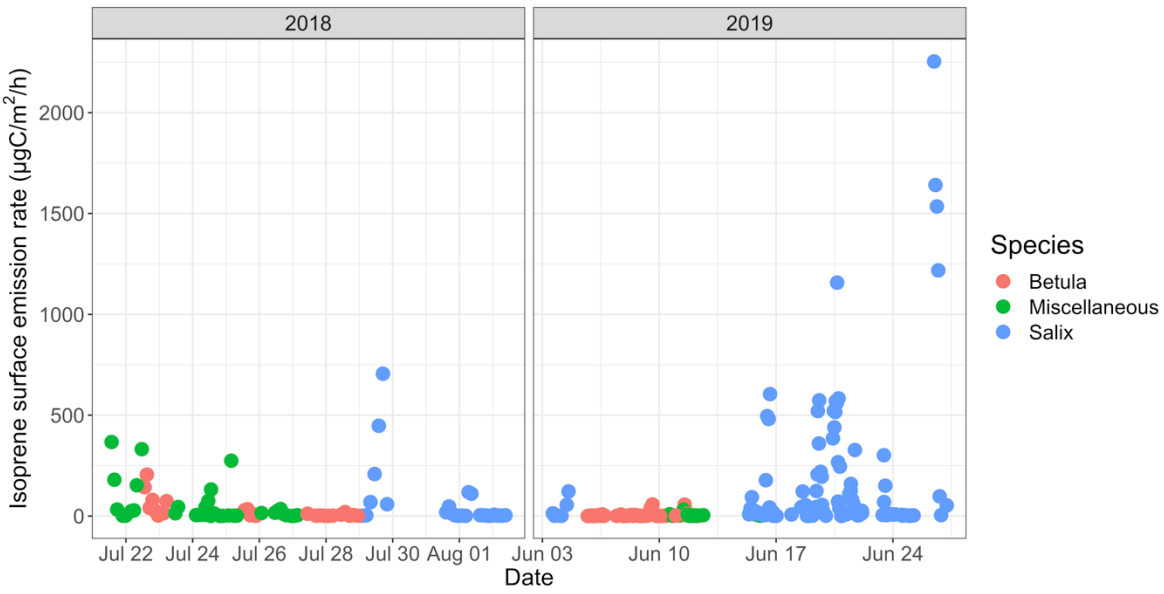

Figure 6: Time-series of isoprene surface emission rates (in µgC/m^2/h) for different vegetation types. Miscellaneous refers to a mix of different species, including lichens and moss tundra.

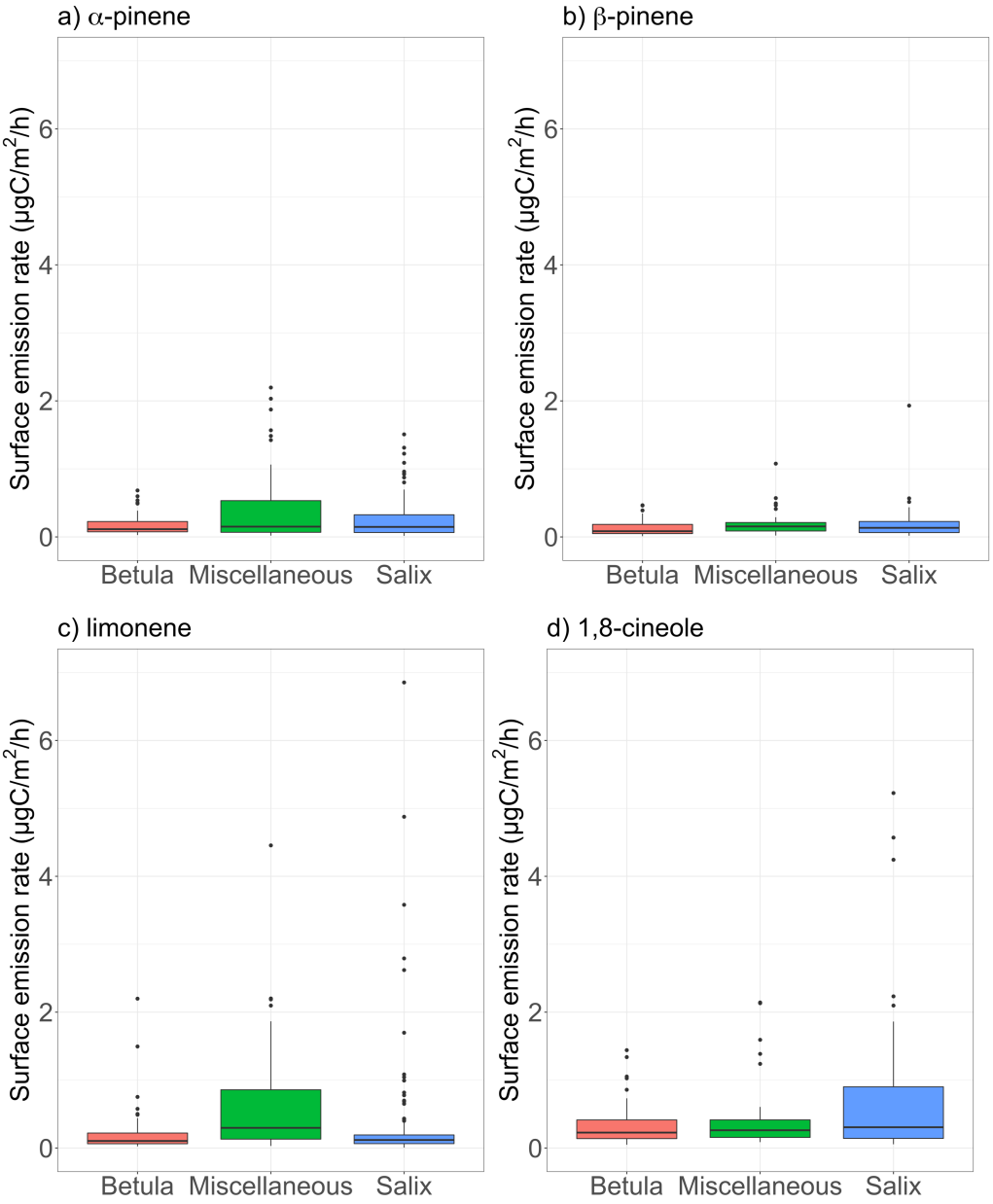

Figure 7: Surface emission rates of various monoterpenes (in µgC/m^2/h) for different vegetation types. The lower and upper hinges correspond to the first and third quartiles. The upper (lower) whisker extends from the hinge to the largest (smallest) value no further than $1.5 \times IQR$ from the hinge, where IQR is the inter-quartile range (i.e., the distance between the first and third quartiles). The notches extend $1.58 \times IQR/\sqrt{n}$ and give a ~95% confidence interval for medians. Miscellaneous refers to a mix of different species, including lichens and moss tundra.

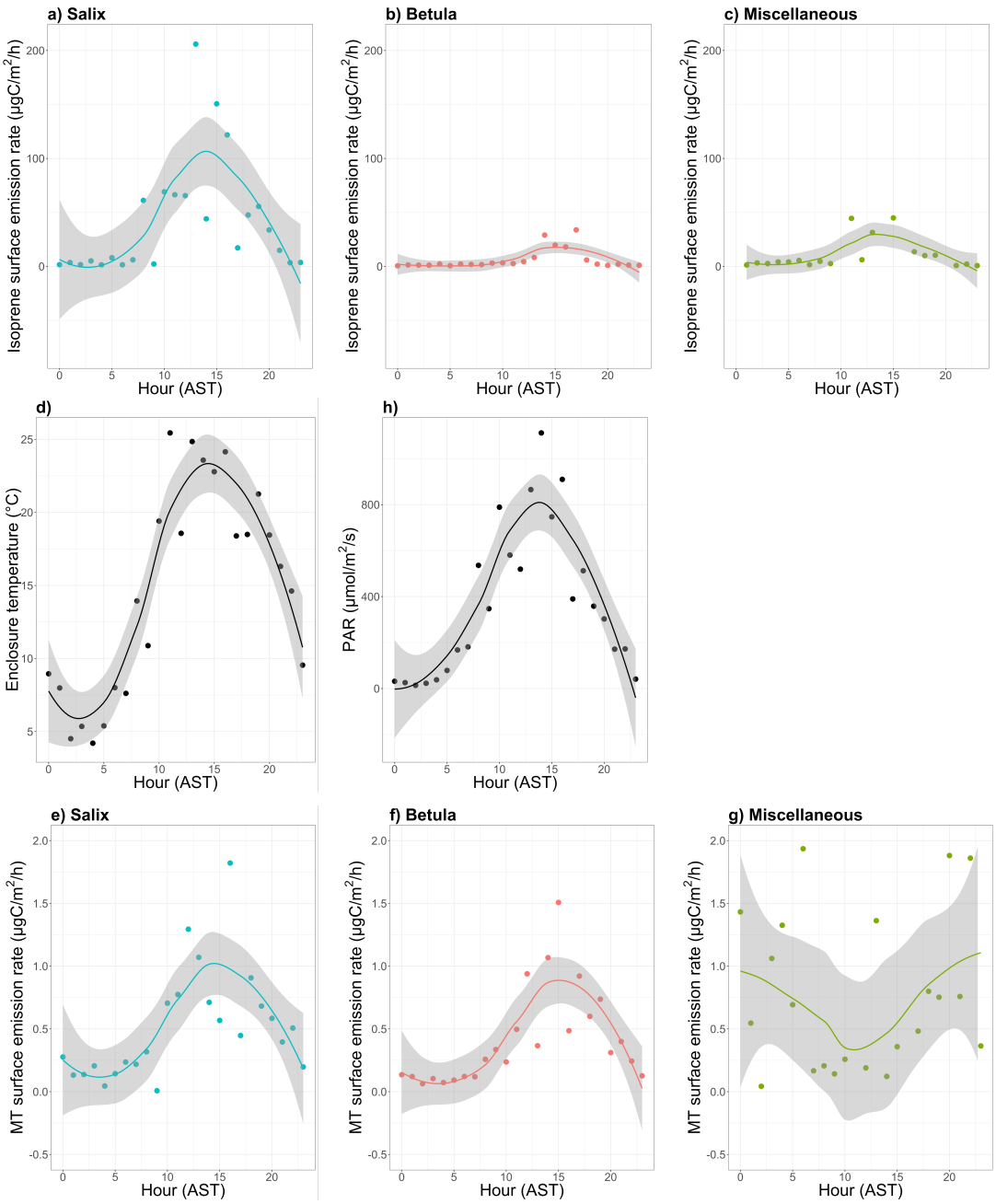

Figure 8: Mean diurnal cycle of isoprene (a-c) and monoterpenes (MT; e-g) surface emission rates (in µgC/m^2/h – note the difference scale on the y-axis), d) enclosure temperature (in °C), and h) enclosure photosynthetically active radiation (PAR in µmol/m^2/s). The dots represent the hourly means. The line is the smoothed conditional mean while the grey shaded region indicates the 95% confidence interval. Hours are in Alaska Standard Time (UTC-9) and correspond to the end of the 2-hr sampling period for isoprene and MT emission rates. MT corresponds here to the sum of α-pinene, β-pinene, limonene, and 1,8-cineole. Miscellaneous refers to a mix of different species, including lichens and moss tundra.

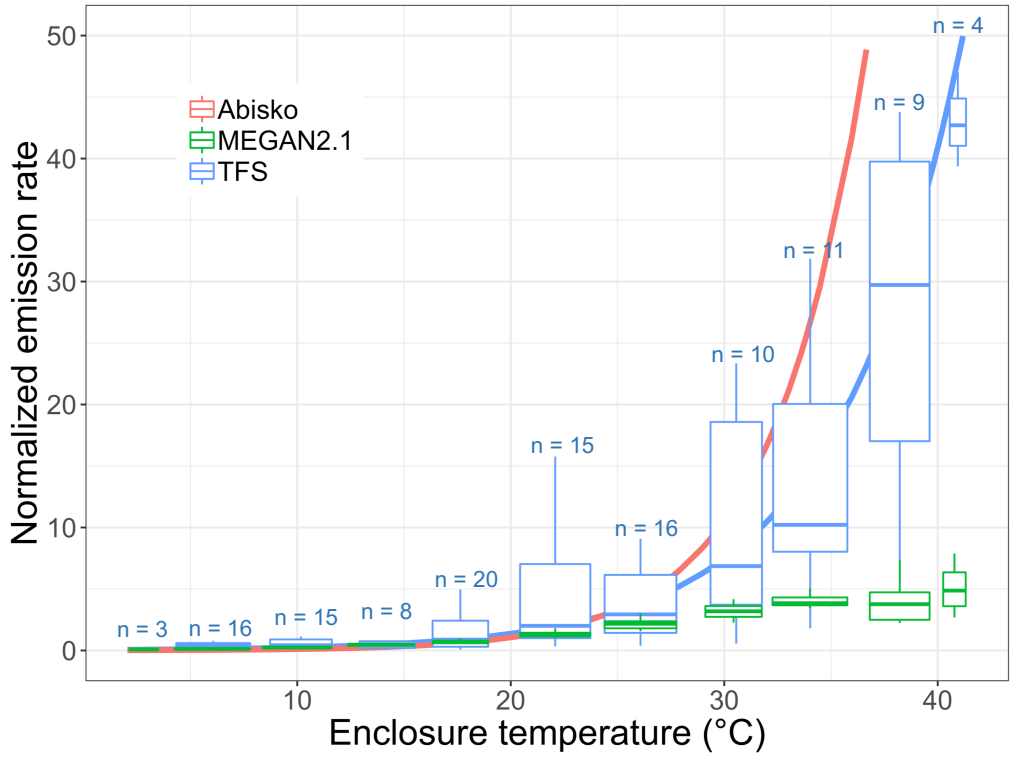

Figure 9: Normalized isoprene surface emission rate (emissions at 20°C set equal to 1.0) as a function of enclosure temperature (in °C). This figure shows the response to temperature as observed at Toolik Field Station (TFS, in blue) and Abisko, Sweden (in pink; Tang et al., 2016), and as parameterized in MEGAN2.1 (in green). The blue solid line is the exponential fit at TFS. n denotes the number of measurements in each enclosure temperature bin. It should be noted that the enclosure temperature was on average 5-6°C warmer than ambient air due to greenhouse heating.